A Landscape Scale Analysis of Vegetation Change within the Blast Zone of the 1980 Mount St. Helens Volcanic Eruption through 2024

by

Alex Burns

A thesis submitted to the Graduate Faculty of
Auburn University
In partial fulfillment of the
requirements for the Degree of
Master of Science

Auburn, Alabama
May 10, 2025

Keywords: Forests, Growth, Height, Multispectral, Spatial, Reforestation

Approved by

Dr. Luke Marzen, Chair, Professor, Department of Geosciences.
Dr. Chandana Mitra, Professor, Department of Geosciences.
Dr. Stephanie Shepherd, Professor, Department of Geosciences.

Abstract

The Mount St. Helens eruption of 1980 resulted in a catastrophic loss of vegetated land within the Pacific Northwest. This study focused on the vegetation throughout the blast zone with a particular interest in comparing vegetation growth patterns on different management areas and exploring environmental drivers of this growth. Using the Normalized Difference Vegetation Index (NDVI) for the years 1984 – 2024 in Emerging Hot Spot Analysis (EHSA), the results showed that vegetation growth was initially greater on properties where there were more remediation efforts following the eruption. In the later years of analysis, the EHSA identified locations on WEYCO where timber harvest was increasing. Therefore, WEYCO is experiencing a more inconsistent rate of growth while NVM continues to have an increase of vegetation growth each year. Multiple Linear Regression analysis (MLR) identified relationships between environmental variables such as slope, hillshade, elevation, and ash depth and vegetation attributes consisting of NDVI and canopy height. This analysis led to the conclusion that areas with greater canopy height and higher NDVI values could be found on steeper slopes with more sunlight exposure and lower initial volcanic ash deposits. These results point towards the potential for greater growth where management is more involved in reforestation efforts in this study area or other similar study areas. Additionally, care should be taken to focus efforts on gentle slopes, higher elevations, or areas where ash is present.

Acknowledgements

First, I would like to thank Dr. Marzen for being a wonderful advisor and professor from whom I have learned much, as well as Dr. Shepherd and Dr. Mitra for being a supportive committee. I admire their work ethic and their individual strengths which I have been a witness to in my time here at Auburn University. This would not be possible without all the valuable feedback I have received from them. I would also like to thank my wife for always supporting me regardless of the endeavor. I am very thankful for her constant encouragement and positivity which often pushes me to finish projects or accomplish goals whether they are big or small. I am also thankful to my family. My siblings have helped me grow over the years, and I will always admire and look up to them. My parents, of course, were a big component of my education prior to college, so I am very thankful for them. I know my mother would be very proud as she oversaw my education at a young age and took pride in teaching my siblings and myself.

Table of Contents

List of Tables

List of Figures

List of Abbreviations

Abbreviation	Definition
ALS	Airborne Laser Scanning
BZ	Blast Zone
CHM	Canopy Height Model
DSM	Digital Surface Model
DTM	Digital Terrain Model
GPNF	Gifford Pinchot National Forest
MSH	Mount St. Helens
NDVI	Normalized Difference Vegetation Index
NVM	National Volcanic Monument
WDNR	Washington Department of Natural Resources
WEYCO	Weyerhaeuser Company

Chapter 1: Introduction

1.0 Background

Mount St. Helens (MSH) is one of several volcanoes that make up the Cascade – Seirra Mountains Physiographic Province that spans the states of California, Washington, Oregon, and continues into Canada *(U.S. Geological Survey, 2023).* The mountain range has long been investigated for the volcanic activity associated with it. The mountains cover an underlying subduction zone where the Juan de Fuca tectonic plate collides with the North American tectonic plate (Decker and Decker, 1981). These plate collisions are related to other plate collisions in what is called the Ring of Fire (Frank et al., 1977). The Ring of Fire surrounds the Pacific Ocean, and it is the boundary where the oceanic tectonic plates are subducted under the continental tectonic plates. These active zones of subduction are known for their association with volcanic activity (National Research Council, 1994). Rich forests surrounded MSH in 1980, and timber harvest was prevalent because of the economic value of materials extracted from the timber. Properties around the volcano were managed by federal and state agencies as well as a private timber corporation. The MSH volcanic eruption of 1980 affected the timber harvest within the blast zone as well as timber growth (Dale et al., 2005). The pyroclastic blast and mudflows resulted in significant destruction, including the loss of approximately 3.2 billion board feet of timber, valued at an estimated $695 million. Most of the damaged timber, around 70%, was privately owned (United States International Trade Commission, 1980). The eruption had effectively erased, not only old timber growth and vegetation on government properties, but younger healthy timber stands occurring on timber company properties as well. The property owners were left to survey the damage and determine what next steps, if any, would be taken to restore the

landscape to its original state.

1.1 Significance

In the Pacific Northwest, 56 million acres are designated as commercial forest lands. The 1977 net sawtimber inventory for the region was nearly 900 billion board feet, representing about 35% of the nation's total sawtimber and 45% of its softwood sawtimber. Most of the commercial forest land is owned by the federal government, followed by industry, private owners, state, and other public entities. From 1960 to 1977, federal and state lands contributed about 45% to 50% of the annual timber harvest, which peaked at 18.8 billion board feet in 1973 before settling at 15.9 billion board feet in 1977 (United States International Trade Commission, 1980). Forests cover approximately 30% of the global land area. Besides providing timber, which contributes substantially to the global economy, forests offer a range of other valuable resources (Whitehead, 2011). Forests and forest products currently offset 12-19% of fossil fuel emissions in the USA (McKinley et al., 2011). Recent studies also show that forests have a positive impact on human health. Forests help in reducing air pollution especially as cities become denser and land for development becomes scarcer. The increase in forested land therefore has a positive relationship with air quality which translates to better cardiovascular and respiratory health (Tan, 2022). Often referred to as nature-based therapy, time spent in a forested environment has also been shown to have a strong impact on mental health. Nature based therapy leads to significant increases in mental well-being among psychosomatic patients, and symptoms of depression decrease significantly for others (Joschko et al., 2023). Approximately 70% of emerging infectious diseases originate in animals. The infections are often linked to the loss of forested area and land-use changes that force human – animal interactions (United Nations,

2021).

Reforestation is the act of restoring forests where tree density and canopy cover have been reduced due to human activities and/or natural disturbances. The reforestation process either occurs naturally or is assisted in some form. Assisting reforestation involves planting more trees in areas where the forest is declining or regenerating degraded forests (Bodo et al., 2021). Reforestation of a landscape is often uneven, with recovery rates typically being slow and emerging forests may not have the same species or provide the same materials and services as previous forests. However, secondary forests can offer crucial environmental services, supporting sustainable development, carbon sequestration, and increased biodiversity (Southworth & Nagendra, 2009). Historically speaking, inside the MSH Blast Zone (BZ) the reforestation efforts vary from assisted recovery to completely natural recovery and anything in between. One common RS approach used in studying landscape scale reforestation involves collecting time-series data over extended periods to monitor changes. The goal of time-series analysis is to quantify the behavior underlying observations, link different observations, and provide insights into the origins of observed phenomena (Lange, 2006). Continuous data products, such as vegetation or spectral indices, emerged to address the limitations of discrete type land cover classification analyses. Rather than categorizing or assigning classes to vegetation in an area, the continuous products yield quantitative measurements for structured analysis of vegetation health. Vegetation indices like the Normalized Difference Vegetation Index (NDVI) are widely used to measure changes in vegetation cover, providing a closer link to land surface processes (Waylen et al., 2014). Remote sensing, particularly using NDVI and other vegetation indices provides consistent, repeatable measurements making it ideal for capturing land surface changes such

as those caused by volcanic activity. If taken properly and during the correct dates, vegetation indices derived from images can measure the extent of increasing or decreasing growth. As remote sensing technology advances, it offers increasing potential for ecological research and monitoring. Predicting the consequences of ecosystem function changes, both natural and human-induced, on landscape scale distributions should be a high research priority, and integrating a full range of remote sensing techniques is important for answering these questions (Kerr & Ostrovsky, 2003).

The satellite imagery available helps analyze vegetation using multispectral data from several bands of the electromagnetic spectrum and this has been the main source of data collected using RS since 1980 at MSH. One of the more recent technologies for collecting RS data is through Light Detection and Ranging (LiDAR). This will be the first study to use LiDAR in a landscape scale analysis at MSH. An analysis of the BZ vegetation using LiDAR will add to previous studies by providing an estimate of tree growth and potentially associated characteristics of tree health that can be derived from tree height. Additionally, spatial analysis techniques using satellite imagery will help analyze the BZ for the years 1984 – 2024. This 40-year collection of satellite imagery has a much greater temporal resolution than any other collection used by other studies at MSH. Additionally, the images will introduce a 30-meter spatial resolution that was not available to studies prior to 1984. The research will add to the knowledge of vegetation reestablishment from previous studies. Knowledge of the growth will help understand the processes of restoration within the BZ and may be used to aid reestablishment in similar areas that have experienced disturbances.

1.2 Study Area

The MSH blast zone covers over 600 km^2 within the Cowlitz, Lewis, and Skamania

counties of southwest Washington. The property ownerships include 171 km^2 of Weyerhaeuser Timber Holdings and 313 km^2 of area around the volcano which has been dedicated as the Mount St. Helens National Volcanic Monument (NVM) (Marzen et al., 2011) (Table 1.1 and Figure 1.2).

Table 1.0: Area for property owners within the blast zone. These values were adapted from Marzen et al. (2011).

Property Owner	Area (km^2)
Washington State	53
GPNF	81
Weyerhaeuser	171
NVM	313
Total	618

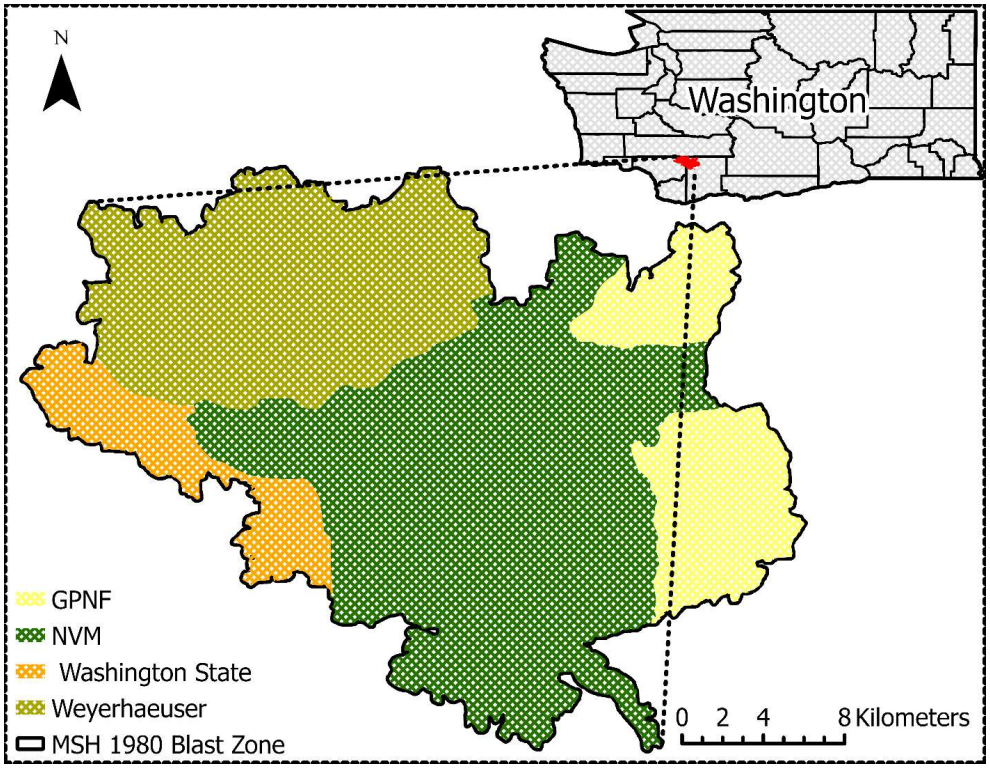

Figure 1.0: This is a map of the blast zone, and the different property owners that lie within it. Between 1980 and 2024 there has been one small change in the property layout. Washington State absorbed 30 km^2 of Weyerhaeuser property (Washington State Geoservices, 2024).

The Gifford Pinchot National Forest (GPNF) management area covers 81 km^2 and is managed for multi-purpose land use including timber operations and recreation. Washington State lands, managed by the Washington Department of Natural Resources (WDNR), are managed for timber production to maximize profit like private lands. Private lands, under Weyerhaeuser Company management, are used primarily for timber operations (Marzen et al., 2011). The Weyerhaeuser Company is an international forest products company with a large focus on timber growth and harvest, and they manage timber stands throughout the U.S. and Canada. Weyerhaeuser has been in the forestry business since 1900, and they established the first certified tree farm in 1941. In the late 1960s, Weyerhaeuser began to practice high yield forestry, which includes environmentally friendly site preparation, vegetation control, hand planting, tree density regulation, and timber harvest scheduling (Heninger et al., 1997). Weyerhaeuser is a large landowner within the blast zone, and the company has played an instrumental role in managing forests in the blast zone.

Post-eruption, the ecosystem began to recover, and management strategies adapted to new environmental hazards and landowners' objectives. Formed in 1980, the St. Helens Forest Lands Research Cooperative held representatives from the DNR, GPNF, and Weyerhaeuser Company properties (Dale et al., 2005). Their goal was to identify major environmental threats post-eruption. They found risks of floods and mudflows from unstable deposits, tephra-covered slopes, dam breaches, and sediment-filled channels. Areas of standing dead trees were seen as susceptible to fires and insect outbreaks which could impact living forests and the salvage potential of timber. The diversity and complexity of these dangers posed significant challenges to resource managers. Aside from the financial

and environmental damage that the eruption created, the eruption formed a unique situation where scientists could study the ability of the landscape to recover following such a large natural disaster. The creation of the Mount St. Helens National Volcanic Monument (NVM) in 1982 was done to preserve the area, ensure safety, and serve as a natural laboratory for land managers and scientists to observe post-eruption changes. The forest service aimed to observe natural geologic and ecological forces within the NVM (Dale et al., 2005).

The understory vegetation was historically diverse, consisting of mosses, herbs, and shrubs. Vegetation types in non-forested areas, such as meadows, wetlands, and avalanche paths, covered about 5% of the area, contributing to the overall biotic diversity. The pre-1980 landscape also exhibited a variety of forest age classes due to wildfires, logging, and volcanic activity (Swanson et al., 2005). The timber species prior to the eruption at MSH consisted of Douglas-fir, Noble Fir, Silver Fir, Western Hemlock, and Western Red Cedar (Snellgrove et al., 1983). At higher elevations, Noble Fir and Silver Fir were the most prevalent (Winjum et al., 1986). Douglas Fir is a species that has grown throughout the region historically (Robbins, 1985). This was one of the species that attracted attention from timber companies long before the eruption, and Weyerhaeuser chose Douglas Fir Seedlings as one of its primary choices for tree farms after the old growth was harvested within the blast zone (Rochelle et al., 1992).

The Pacific Northwest region, particularly around Mount St. Helens, experiences significant climate variations influenced by the Pacific Ocean and the north-south Cascade Range. Moisture decreases from west to east but increases with elevation, while temperatures decrease with elevation. The area has mild, wet winters and warm, dry summers. Spirit Lake, at an elevation of 988 meters, receives an average annual

precipitation of 2373 mm, with most of it falling outside the Summer Months. Precipitation below 600 meters falls mainly as rain, whereas elevations above 1000 meters see seasonal snowpacks (Swanson et al., 2005). Elevations within the blast zone range from 330 to 2540 meters above sea level. Soils within BZ consist of the soil orders Alfisols, Entisols, Inceptisols, Mollisols, Ultisols, and Spodosols. Spodosols being the majority covering 44% of the BZ (United States Department of Agriculture, 2016).

1.3 Research Objectives

Objective 1

This study aims to accomplish three objectives. The first objective is to track the recovery of vegetated and forested areas throughout the years 1984 – 2024. Various studies have completed time series analysis of the vegetation recovery within the blast zone, but no study has completed an analysis of images for every year between 1984 and 2024. Additionally, this study will implement Emerging Hot Spot Analysis which is a 3 – dimensional space - time analysis (Ghanghermeh et al., 2024). Utilizing vegetation index images derived from optical imagery, the completion of this objective would effectively determine the growth of vegetation in the various management areas in the BZ.

Completing Objective 1 will answer the first research question:

Q1. How has vegetation been reestablished in the various management areas in the blast zone over the past 40 years?

Objective 2

Objective 2 is to use available LiDAR derived data to develop a CHM for the study area which allows for comparison of canopy height on all four of the defined management areas.

Completing Objective 2 will answer the following research question:

Q2. What is the relative canopy height in each management area as determined by ALS derived data?

Objective 3

The final objective is to utilize canopy height information as well as NDVI values gathered in the same year to explore variables that have influenced the reestablishment of the vegetated and forested areas. Independent variables such as elevation, slope, ash depth, and hill shade will be tested against canopy height and the NDVI values in regression analysis.

Completing Objective 3 will answer the final research question:

Q3. What environmental variables were the drivers of reestablishment?

Organization of Study

The thesis is organized into **four (4)** chapters. **Chapter 1** provides an introduction and the significance of the study as well the study area and objectives. **Chapter 2** presents a review of literature which is relevant to the study or study area and its relevance to the study. **Chapter 3** Introduces the NDVI time series analysis including emerging hotspot analysis of the revegetation and reforestation of the BZ over the years 1984 – 2024. **Chapter 4** will introduce ALS to the study which includes the results of height analysis and the regression analysis of the relationship between independent environmental variables to the dependent variable(s) of canopy height and NDVI. **Chapters 3 and 4** are being prepared for publication in scientific journals. These chapters are written in this thesis as standalone chapters as they would appear in a journal submission. **Chapter 5** summarizes the findings of the work and introduces suggestions for future work.

1.4 References

Bodo, T., Gimah, B. G., & Seomoni, K. J. (2021). Deforestation and habitat loss: Human causes, consequences and possible solutions. *Journal of Geographical Research*, *4*(2), 22–30. https://doi.org/10.30564/jgr.v4i2.3059

Chakravarty, S., K., S., P., C., N., A., & Shukl, G. (2012). Deforestation: Causes, effects and Control Strategies. *Global Perspectives on Sustainable Forest Management*. https://doi.org/10.5772/33342

Dale, V. H., Swanson, F. J., & Crisafulli, C. M. (2005). Ecological Perspectives on management of the mount st. helens landscape. *Ecological Responses to the 1980 Eruption of Mount St. Helens*, 277–286. https://doi.org/10.1007/0-387-28150-9_19

Decker, R., & Decker, B. (1981). The Eruptions of Mount St. Helens. *Scientific American*, *244*(3), 68–81. http://www.jstor.org/stable/24964328

Fahey, T. J., Woodbury, P. B., Battles, J. J., Goodale, C. L., Hamburg, S. P., Ollinger, S. V., & Woodall, C. W. (2009). Forest Carbon Storage: Ecology, management, and policy. *Frontiers in Ecology and the Environment*, *8*(5), 245–252. https://doi.org/10.1890/080169

Frank, D., Meier, M. F., Swanson, D. A., with contributions by Babcock, J. W., Fretwell, M. O., Malone, S. D., Rosenfeld, C. L., Shreve, R. L., & Wilcox, R. E. (1977). Assessment of increased thermal activity at Mount Baker, Washington, March 1975-March 1976. *Professional Paper*. https://doi.org/10.3133/pp1022a

Grassi, G., House, J., Dentener, F., Federici, S., den Elzen, M., & Penman, J. (2017). The key role of forests in meeting climate targets requires science for credible mitigation. *Nature Climate Change*, *7*(3), 220–226. https://doi.org/10.1038/nclimate3227

Ghanghermeh, A., Roshan, G., Asadi, K., & Attia, S. (2024). Spatiotemporal analysis of urban heat islands and vegetation cover using emerging hotspot analysis in a humid subtropical climate. *Atmosphere*, *15*(2), 161. https://doi.org/10.3390/atmos15020161

Heninger, R. L., Terry, T. A., Dobkowski, A., & Scott, W. (1997). Managing for sustainable site productivity: Weyerhaeuser's Forestry Perspective. *Biomass and Bioenergy*, *13*(4–5), 255–267. https://doi.org/10.1016/s0961-9534(97)10013-7

Joschko, L., Pálsdóttir, A. M., Grahn, P., & Hinse, M. (2023). Nature-based therapy in individuals with mental health disorders, with a focus on mental well-being and connectedness to nature—a pilot study. *International Journal of Environmental Research and Public Health*, *20*(3), 2167. https://doi.org/10.3390/ijerph20032167

Kerr, J. T., & Ostrovsky, M. (2003). From space to species: Ecological applications for remote sensing. *Trends in Ecology & Evolution*, *18*(6), 299–305. https://doi.org/10.1016/s0169-5347(03)00071-5

Lange, H. (2006). Time-series analysis in Ecology. *Encyclopedia of Life Sciences*. https://doi.org/10.1038/npg.els.0003276

Marzen, L. J., Szantoi, Z., Harrington, L. M. B., & Harrington, J. A. (2011). Implications of management strategies and vegetation change in the mount st. helens blast zone. *Geocarto International*, *26*(5), 359–376. https://doi.org/10.1080/10106049.2011.584977

McKinley, D. C., Ryan, M. G., Birdsey, R. A., Giardina, C. P., Harmon, M. E., Heath, L. S., Houghton, R. A., Jackson, R. B., Morrison, J. F., Murray, B. C., Pataki, D. E., & Skog, K. E. (2011a). A synthesis of current knowledge on forests and carbon storage in the United States. *Ecological Applications*, *21*(6), 1902–1924. https://doi.org/10.1890/10-0697.1

National Research Council. (1994). *Mount Rainier: Active Cascade Volcano*. Washington, DC: The National Academies Press. https://doi.org/10.17226/4546.

Robbins, W. G. (1985). The social context of forestry: The Pacific Northwest in the Twentieth Century. *The Western Historical Quarterly*, *16*(4), 413. https://doi.org/10.2307/968606

Rochelle, J. A., Ford, R. L., & Terry, T. A. (1992). The Reforestation Challenge. *Journal of Forestry*, *90*(5), 20–24. https://doi.org/10.1093/jof/90.5.20

Snellgrove, T. A., Kendall Snell, J. A., & Max, T. A. (1983). Damage to national forest timber on Mount St. Helens. *Journal of Forestry*, *81*(6), 368–371. https://doi.org/10.1093/jof/81.6.368

Southworth, J., & Nagendra, H. (2009). Reforestation: Challenges and themes in reforestation research. *Landscape Series*, 1–14. https://doi.org/10.1007/978-1-4020-9656-3_1

Swanson, F. J., Crisafulli, C. M., & Yamaguchi, D. K. (2005). Geological and ecological settings of Mount St. Helens before May 18, 1980. *Ecological Responses to the 1980 Eruption of Mount St. Helens*, 13–26. https://doi.org/10.1007/0-387-28150-9_2

SZABÓ, P. (2010). Why history matters in ecology: An interdisciplinary perspective. *Environmental Conservation*, *37*(4), 380–387. https://doi.org/10.1017/s0376892910000718

Tan, B. Y. (2022). Save a tree and save a life: Estimating the health benefits of urban forests. *Environmental and Resource Economics*, *82*(3), 657–680. https://doi.org/10.1007/s10640-022-00677-y

Troll, C. (1939). Luftbiltplan und okologische Bodenforschung. *Z. Ges. f. Erdkunde z. Berlin, kundliches Wissen*, *3*, 241-311.

United Nations. (2021). *Forest restoration: A path to recovery and well-being*. https://www.un.org/en/un-chronicle/forest-restoration-path-recovery-and-well-being-0

United States Department of Agriculture. (2016). *Washington State General Soil Map*. Web soil survey. https://websoilsurvey.sc.egov.usda.gov/App/WebSoilSurvey.aspx. Accessed [2/12/2025]

United States Department of Agriculture. (n.d.). *Spodosols*. Natural Resources Conservation Service. https://www.nrcs.usda.gov/conservation-basics/natural-resource-concerns/soils/spodosols Accessed [2/12/2025]

von Holle, B., Yelenik, S., & Gornish, E. S. (2020). Restoration at the landscape scale as a means of mitigation and adaptation to climate change. *Current Landscape Ecology Reports*, *5*(3), 85–97. https://doi.org/10.1007/s40823-020-00056-7

Washington State Geoservices. (2024). *Current parcels*. https://geo.wa.gov/datasets/wa-geoservices::current-parcels/about Accessed [2/12/2025]

Whitehead, D. (2011). Forests as carbon sinks--benefits and consequences. *Tree Physiology*, *31*(9), 893–902. https://doi.org/10.1093/treephys/tpr063

Waylen, P., Southworth, J., Gibbes, C., & Tsai, H. (2014). Time series analysis of land cover change: Developing statistical tools to determine significance of land cover changes in persistence analyses. *Remote Sensing*, *6*(5), 4473–4497. https://doi.org/10.3390/rs6054473

Yu, H., Liu, X., Kong, B., Li, R., & Wang, G. (2019). Landscape Ecology Development supported by Geospatial Technologies: A Review. *Ecological Informatics*, *51*, 185–192. https://doi.org/10.1016/j.ecoinf.2019.03.006

Chapter 2: Literature Review

2.0 Volcanic Activity in The Pacific Northwest

The United States Geological Survey (USGS) was aware of the increase in activity from Mount St. Helens (MSH) well before the 1980 eruption occurred. In the 1970s, seismic monitoring was established at the volcano, and it became more of a focus in early 1980 as volcanic activity increased. USGS Scientists used early Global Positioning System (GPS) technology to measure ground deformation which was the first sign of a lateral blast. Using GPS technology in combination with tiltmeters, the USGS detected the bulging of the north flank of the volcano (USGS, 2023). On May 18th, the eruption began with a 5.1 magnitude earthquake at 8:32 am which triggered a large landslide followed by the lateral blast from the north flank destroying the land to the north of the volcano (Figure 2.0).

Figure 2.0: The photo on the left was captured over Spirit Lake in the BZ prior to the eruption in the spring of 1980. From WDNR (2017). The photo on the right was captured in 1984, and it shows the surroundings of Spirit Lake following the 1980 eruption. Notice the divers in Spirit Lake studying the damage done to the lake. Taken from Austin (1986).

Continuing for nine hours, the blast was so large that pyroclastic flows, lahars, and ashfall affected 11 U.S. States. It not only devastated much of the natural environment, destroying vegetation, but there were also 57 lives lost in total in both the immediate and surrounding areas due to the eruption events (USGS, 1981)

The geologic record shows that MSH has one of the most comprehensive eruption histories of any volcano within the United States (Decker and Decker, 1981). The Volcano remains active today and has even produced another eruption from 2004 – 2008. During the prolonged eruption, a new dome was built up in the middle of the crater of the 1980 eruption (USGS, 2023). On Oct. 30, 2023, USGS scientists at the Cascades Volcano Observatory released a report stating "In late August to early September, about 40-50 earthquakes were located per week, and more recently, the number has been about 30 located earthquakes per week. To compare, since 2008, on average about 11 earthquakes have been located per month at Mount St. Helens." In this report, no other changes were noted at other volcanoes in the Cascade Range (USGS, 2023). Other volcanoes in the area consist of Mount Rainier, Mount Baker, and Mount Adams. Frank et al. (1977) was studying Mount Baker and its increase in thermal emissions only a few years prior to the eruption at MSH. Mount Rainier had a long eruptive history at the time of the 1980 eruption at MSH, and it is still being closely watched (National Research Council, 1994). In response to the MSH 1980 eruption, the USGS expanded its team, deployed new instruments, developed forecasting tools, and improved communication pathways. With the knowledge and experience gained from volcanic activity in the area, the USGS developed the Volcanic Risk Management System (VRMS). This system involves coordination and effective exchange of hazard and

risk information among other scientists, emergency managers, policymakers, and communities (Wright et al. 2023). The VRMS would help prevent some of the more critical issues that occurred during the MSH eruption such as the loss of property and life.

2.1 Early Field Studies Surveying the Impact in The MSH Blast Zone

Plant succession at MSH directly following the 1980 eruption was believed to be a mix of both primary and secondary succession (Moral et al., 2007). Primary succession takes place when growth occurs in areas such as barren rock with no soil presence whereas secondary succession occurs in more likely areas that have nutrient rich soil. Initial responses of plant and tree species on the ground ranged from complete devastation to some survival of various species in many locations. Weathering of sediment and other secondary disturbances following the eruption influenced recovery and reestablishment (Dale et al., 2005). Primary succession was believed to have progressed slowly due to erosion, lack of soil nutrients, and soil surface drought (Moral & Wood, 1993). Species survived in various ways. In some cases, roots were preserved underground and in areas the ash deposits were thin enough for life to escape. It was believed that one of the most important variables in recovery was the simple matter of whether there were any plants or life left in the vicinity to produce other life. It was also believed that the time of the year saved many species. With the blast occurring in May, there was some snow on the ground, and the preceding months were more friendly to plant growth than winter would have been. Some of the earliest surviving plant and tree species included Fireweed, Thistle, Western Hemlock, and Pacific Silver Fir (Franklin, 1990). Many plant and animal groups survived and were well dispersed throughout the affected area, providing sources of vegetative regrowth and seed production. Seed dispersal from adjacent undamaged regions played a significant role in

early reestablishment (Franklin et al. 1988).

Ecologists saw the post eruption blast zone as a slate wiped clean which gives an opportunity to study the re-establishment of various species of vegetation (Dale and Crisafulli, 2018). Halpern et al. (1990) studied the area directly following the eruption and reinforced the suggestion that the destruction caused to vegetation could be placed into one of four broad groups following the eruption: uprooted forests; uprooted forests covered in snow; standing forests effected by heat; and areas that were cleared by timber companies prior to the eruption. Halpern et al. (1990) found that the early plant succession in areas of blown-down and scorched forests in the blast zone was often influenced by secondary disturbance occurring after the eruption. Despite some of the plots showing rapid plant cover increase, most sites remained barren, with an average plant cover of less than 10% after seven growing seasons. Initial survival was highest in areas with a snowpack during the eruption, which protected plants and facilitated their emergence (Figure 2.1)

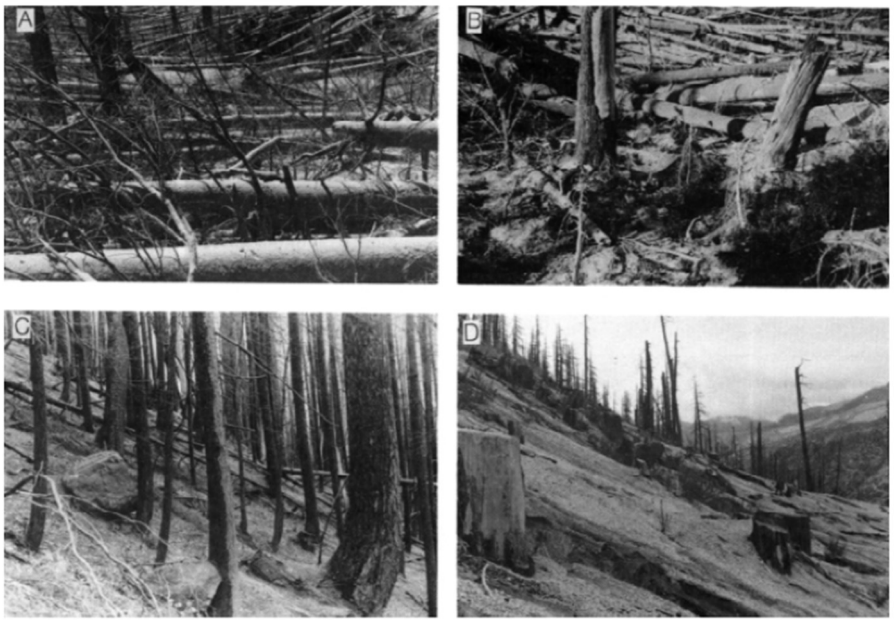

Figure 2.1: Halpern (1990) photographed timber in four physical states following the eruption in 1980; blown down timber (A), blown down timber with snowpack (B), standing burnt timber (C), and timber that was clear cut prior to the eruption (D).

Twenty-six years later, species diversity had increased, and the growth rates remained the same. The recovery process was seen as slow and plant cover averaged around 50% in the National Volcanic Monument (NVM). Forest within the NVM was nonexistent, but it was expected that coniferous trees would soon recolonize at an exponential rate providing seeds for each other (Cook & Halpern, 2018). Long-term monitoring on the ground continues to bring about surprises to ecologists. Many concepts of succession have failed to apply in the blast zone, but others have proven to be valid. Ecologists pointed out that twenty years of recovery was just the beginning, and more was likely to be learned (Lovett, 2000). Even one ecologist with fifty years' experience claimed they are still learning from succession at MSH (Nash, 2010).

2.2 Importance of Forest Management

The Pacific Northwest is packed with dense evergreen coniferous forests which are known for the massive size and longevity of their trees. Washington itself has over 22 million acres of forested land (Azuma et al., 2006). There is a larger accumulation in the Pacific Northwest, and it lies in the growth of the dominant conifer species. The conifer dominance in the Pacific Northwest is believed to be a product of their ability to photosynthesize year-round, the individual tree size, and their resilience to environmental stresses. Douglas fir, a species native to the area, initially grows slower than the pine species present in the southeastern U.S. but eventually surpasses it in size. If properly managed, a 100-year forest stand of Douglas Fir can produce as much as 22% more above ground biomass than two 50-year forest stands of the southeastern species of pines (Waring & Franklin, 1979).

A well-managed forest provides habitat for wildlife, enhances environmental quality,

and reduces the risk of wildfire and disease. Proper management to promote a healthier forest involves manipulating species composition, stand structure, and tree numbers through cutting selected trees and understory vegetation. Forest management is essential due to the changing nature of forests in modern times (USDA, 2023). Understory vegetation plays a vital role in maintaining forest biodiversity which makes it high in forest management priorities from timber production to overall forest quality. The primary goal of forest management is to balance the upper canopy and understory vegetation. Forest management practices such as clear-cutting, and thinning affect understory vegetation. Most often, these practices can enhance understory species, but they may also reduce species diversity (Chen et al., 2025). Research generally supports the idea that increasing plantation style forests can reduce pressure on natural forests mainly for the reason of timber production. This is a hypothesis commonly referred to as the plantation conservation benefit. Forests planted for timber production reduce the rate of degradation to natural and old growth forests (Pirard et al., 2016).

2.3 Forest Management Following the Eruption

Marzen et al. (2011) defined each property within the Blast Zone (BZ)as a management area because the different properties had very different management strategies following the eruption. The property managers interested in harvesting timber, focused on managing for optimized timber growth. Some of the other properties were mandated by law to allow vegetation to recover from natural processes which would lead to slower reestablishment. The National Volcanic Monument (NVM) allowed for natural ecological recovery. The Gifford Pinchot National Forest (GPNF) underwent salvage logging and replanting with conifer species. Private forestlands under Weyerhaeuser Company (WEYCO) were logged

and replanted (Lawrence, 2005). The reforestation efforts following the MSH eruption were based on decades of forestry research and operational experience for Weyerhaeuser. Studies in regeneration ecology, forest soil productivity, and managed-stand growth provided the scientific foundation for subsequent soil management and regeneration practices (Snellgrove et al., 1983). WEYCO faced the challenge of salvaging and reforesting the damaged areas quickly and effectively. The company began salvage operations in the fall of 1980 to recover 850 million board feet of timber over the next 26 months. The reforestation efforts involved planting 18.4 million trees on more than 184 km^2 of different properties, utilizing effective site preparation techniques like slash burning and scarification to expose mineral soil to plant. Human intervention, in conjunction with natural processes, played a crucial role in enhancing ecological recovery post-eruption. Salvage logging, site preparation, and planting accelerated the reduction of erosion and facilitated the establishment of native vegetation (Rochelle et al., 1992). Salvage logging was a major focus considering the amount of blown down timber (Figure 2.2).

Figure 2.2: This picture helps readers to better grasp the destruction which was cast upon the timber in the BZ. The image was taken once the Weyerhaeuser company was allowed to begin salvage logging operations in the fall of 1980. The blown down forest stand in the background was 90 years old. Taken from Rochelle et al. (1992).

WEYCO planted a variety of tree species as part of their reforestation efforts following the eruption. Douglas Fir was planted below 914 meters of elevation while Noble Fir was planted above 914 meters (Rochelle et al., 1992, Marzen et al., 2011). Both tree species were naturally occurring in the area prior to the eruption, and they were strategically chosen based on their suitability for different elevations and environmental conditions to promote successful reforestation and ecosystem recovery. Other species were planted in suitable areas including lodgepole pine and black cottonwood. Fertilization significantly enhanced the total height growth and diameter growth of forest seedlings but reduced their

survival rates (Franklin, 1990) (Figure 2.3).

Figure 2.3: This is a photograph of a Weyerhaeuser employee planting seedlings in the MSH BZ sometime after salvage logging was complete. Weyerhaeuser, the company, took place in salvage logging and replanting on several properties other than its own. Taken from Winjum et al. (1986).

According to Winjum et al. (1986), WEYCO property had replanted over 162 km^2, Washington State property had replanted roughly 20 km^2, and GPNF had replanted roughly 57 km^2 within the first five years following the eruption. Following its designation as a National Monument, there were no replanting or salvage operations within the NVM. Human activities outside the NVM accelerated the recovery of areas affected by eruption. Tree planting significantly contributed to the rapid reestablishment of forests, but natural recovery within the NVM is believed to continue to be a slow and complex process.

Controversies over restoration measures at MSH have focused on the potential negative effects on non-target organisms or processes, and potential loss of scientific value. The establishment of the NVM resolved many issues related to scientific value by substantially limiting human access and activity on the monument lands (Franklin et al., 1988).

2.4 Remote Sensing

RS is the acquisition of information about a phenomenon by a sensor not in direct physical contact with it. RS techniques are classified as passive or active. Passive sensors respond to natural radiation sources while active sensors generate and receive their own radiation. RS first became successful for scientific use when satellites and their sensors began providing valuable information in meteorology. The benefits of satellites in meteorology were that they provided a bird's eye view to cloud systems over very large areas. Since, this type of imagery has become invaluable for weather forecasting (Cracknell, 2018).

RS analysis would not be possible without a Geographic Information System (GIS). GIS is made of several components, including data, people, hardware, and software. GIS fulfills functions such as data collection, data management, data processing, data analysis, and data visualization, and it is useful for many spatial studies including those which involve remotely sensed data. While computer generated maps were created prior to 1969, the Institute of Environmental Systems Research (ESRI) introduced the first version of the ArcInfo program in the 1980s. ArcInfo was one of many GIS platforms that had become available in the early 1980's. ESRI has since replaced ArcInfo with its more advanced GIS ArcMap and ArcPro (Mierzejowska & Żogała, 2018).

In 1972, NASA launched Landsat-1. This was the first satellite of many for the Landsat

program. The Landsat program has captured millions of images over the years. There have since been 7 additional Landsat satellites launched with varying characteristics and lengths of operation. Landsat captured images of the surrounding environment from before and after the 1980 MSH eruption (USGS, 2024). RS has been found useful for inventorying resources and helping to investigate ecological problems in a cost effective and timely manner (Parece, 2015). Remote sensors on satellites like the Landsat series are powerful tools for monitoring the Earth's surface and atmosphere at various scales, providing crucial coverage, mapping, and classification of land cover and associated land uses (Al-Wassai & Kalyankar, 2013). Satellites with Multispectral sensors can collect a large amount of data at a regional scale in a small amount of time and the sensors can detect characteristics that the human eye could not typically perceive because they measure energy in wavelengths outside those of the typical visible spectrum (Kerr and Ostrovsky 2003).

RS data are often utilized for various applications based on spatial, temporal, spectral, and radiometric resolutions. Spatial resolution refers to the smallest object a sensor can separate amid pixels in a digital image. Higher spatial resolution means more pixels or cells per unit area which leads to more detailed information. Temporal resolution represents how frequently measurements are taken. The temporal resolution is dependent on the sensor's ability to make measurements over time. Spectral resolution is determined by the number of spectral bands a sensor measures reflectance. Radiometric resolution is the ability of the sensor to record higher or lower output values in the data (Efremenko & Kokhanovsky, 2021). Higher resolution images can capture more detailed information while lower resolution images tend to over generalize the phenomenon being recorded. This overgeneralization, often referred to as the Modifiable Areal Unit Problem (MAUP),

can become an issue when the spatial resolution is not appropriate for the scale of the study (Jelinski & Wu, 1996). Additionally, using higher spatial resolution to record information in a study area will allow for a more precise analysis (Figure 2.4).

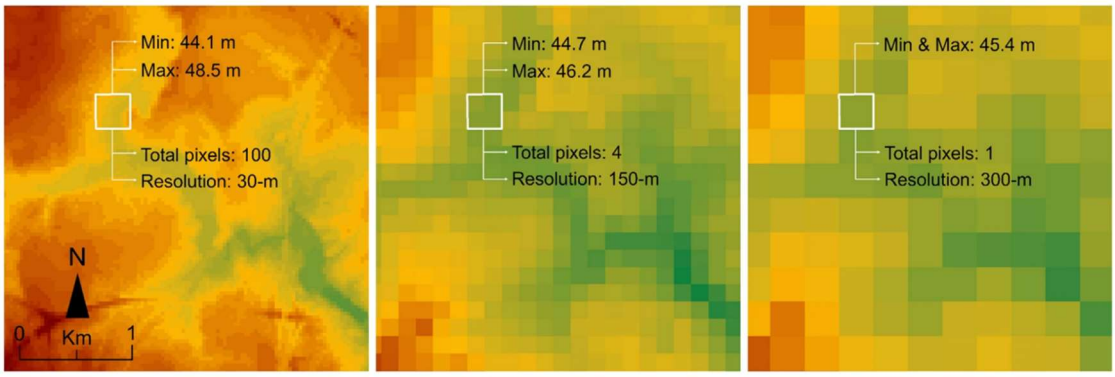

Figure 2.4: A visual representation of the benefits of using higher resolution spatial data. Each pixel holds a value. Finer resolution allows for more of these values to be stored and limits the over generalization that occurs when using a lower resolution. From Markham et al. (2022).

The spatial resolution of the data for spatial studies conducted in the blast zone has become higher with more recent studies. Lawrence and Ripple (1998) and Marzen et al. (2011) conducted analysis using finer resolution (30m) which improved upon their previous study which was using imagery with 80m resolution (Harrington et al. (1998),. Teltscher and Fassnacht (2018) have introduced 10m resolution imagery from the Sentinel satellites to study the blast zone. The increase in resolution as technology advances is helpful as studies utilizing higher resolution data can gather more information about the MSH blast zone.

2.5 Remote Sensing For Forests – NDVI

Vegetation indices are quantitative RS measurements that indicate the vigor and overall health of vegetation. The more complex indices, being combinations of multiple bands, offer more sensitivity for vegetation detection compared to individual bands gathered from a multispectral image. Vegetation indices are commonly used to measure and monitor land

use change detection, forestry, and agriculture (Bannari et al., 1995). Many studies use vegetation indices in these situations to observe the phenology of vegetation and forests which is the seasonal occurrence of vegetation growth or loss (Denny et al., 2014). The Normalized Difference Vegetation Index (NDVI) is a common vegetation index used for measuring phenology. It is used to determine the extent of tree leaf growth or plant growth in the spring as well as the loss of leaves or vegetation in the fall (Peng et al., 2017). The NDVI was found useful for vegetation analysis once multispectral data became available and has been very important to study vegetation at the landscape scale directly following the eruption of 1980. The NDVI was used by Marzen et al. (2011), Lawrence and Ripple (1998), and Harrington et al. (1998) papers, for qualitative and quantitative analysis of vegetation health after the 1980 eruption. These studies chose anniversary dates for time series analysis. Choosing summer dates for every image allowed for the measurement of growth in each year without the issues of snow in winter months and inconsistent leaf loss or gain in the fall and spring months.

Wang et al. (2010) reviewed multiple remote sensing indices valuable to both spatial scientists and ecologists. In their discussion of vegetation indices, they point out that the NDVI has been used in multiple studies to great success. Huang et al. (2020) stated that "The Normalized Difference Vegetation Index (NDVI), one of the earliest remote sensing analytical products used to simplify the complexities of multi-spectral imagery, is now the most popular index used for vegetation assessment." NDVI derived from Landsat images is a valuable resource for measuring forest and vegetation health and is often used in combination with LiDAR for above ground biomass estimations. To improve accuracy of measuring forest health, it is suggested that an NDVI time-series of images provides better

results than a single NDVI image. While optical imagery typically has lower accuracy for forest health measurements when compared to LiDAR, optical imagery is typically more readily available and has a higher temporal resolution (Zhu & Liu, 2015). The NDVI is calculated using Near InfraRed (NIR) and Red wavelengths (Figure 2.5).

$$NDVI = \frac{NIR - Red}{NIR + Red}$$

Figure 2.5: The equation for NDVI calculation. This calculation occurs on a cell-by-cell basis in an image converting cells in a multispectral image into an NDVI image which represents valuable information about forest health.

Healthy vegetation shows high reflectance values for the NIR spectrum, while also absorbing visible red light. Meaningful output values with respect to vegetation from NDVI typically range from 0 to 1.0.

2.6 Remote Sensing For Forests – LiDAR

Light Detection And Ranging (LiDAR) is an RS method used for acquiring high-density and high-accuracy spatial data. In its simplest form, LiDAR uses laser pulses to measure distances using the reflections or returns of the laser pulses. LiDAR records the X, Y, and Z coordinates of the features as they encounter them from the interaction on the surface. Travel time of the laser is used to record X and Y locations as well as the elevation or Z value providing 3D measurements of the area (Wang et al., 2020). Airborne Laser Scanning (ALS) uses a LiDAR system mounted on an aircraft. The system emits laser pulses towards the ground. These pulses reflect off objects such as trees, buildings, and the terrain and are detected by the LiDAR sensor. The first return or pulse is generally a tree or

man-made object while the last return or pulse is from the laser reaching the ground. By measuring the time it takes for the laser pulses to travel to the ground and back, the system calculates the distance between the aircraft and the ground. The aircraft's position and orientation are tracked using GPS and an Inertial Measurement Unit (IMU) (Wehr & Lohr, 1999).

ALS is a popular use for LiDAR especially for forestry and vegetation management applications. Forest stand age serves as an indicator of forest stand quality, and more mature forest stands tend to be less diverse with height being a primary indicator of the age (Racine et al. 2014). Racine et al. (2021) utilized ALS to estimate forest stand age by finding forest structure and site attributes in Quebec, Canada. The study identified distinct patterns among different species, and they found that stands of the same species share similar height characteristics which aid in species classification using ALS. The study also highlighted the impact of crown cover and age on the vertical distribution. Increased crown cover and greater height returns indicated an older forest stand. ALS has traditionally been relatively expensive to collect and requires a specialized platform for the collection process. It is now more common for studies to conduct research using ALS data. As technology has advanced, government organizations have collaborated to make ALS data available in the public domain making more investigations possible (Oh et al., 2022). Many Unmanned Aerial Systems (UAS) companies also offer UAS packages with LiDAR systems (Pricope & Bashit, 2023).

2.7 Remote Sensing Studies in The MSH BZ

There have been multiple remote sensing studies in the MSH BZ with interests in monitoring every aspect of the landscape including vegetation, wildlife, and volcanic activity. In a study monitoring the eruptive activity in the early 2000's, researchers used thermal imaging to measure and analyze the surface temperatures of the volcanic dome. On October 14, 2004, the highest temperature measured at the dome was 675°C. LiDAR data from 2003 and 2004 were also used to create shaded relief and topographical images of the volcanoes' dome before and after the 2004 eruption. The study demonstrated the value of multispectral imagery and LiDAR data for volcano monitoring and the importance of ALS in evaluating changes in the dome of a volcano (Vaughan et al., 2005).

Another study used GIS and RS for evaluating wildlife habitat quality. The study found that, in the years following the 1980 eruption of MSH, the population of Columbian black-tailed deer declined. The study used six dates of post-eruption Landsat imagery including the years 1984, 1988, 1991, 1996, 1999, and 2002 to quantify landscape forage conditions and relate them to the deer population changes. Vegetation maps placed into a GIS model estimated the highest population that would be supported based on the nutrient and food estimates of the vegetation (Davis et al., 2010).

Rogic et al. (2023) used radar backscatter data at MSH to map volcanic flow deposits. Using dual-band radar data, a method was developed to extract surface roughness from the dual-band radar data. The radar data was calibrated using ALS derived digital surface models. The authors found that rough surface features, such as hummocky debris avalanche deposits, could be identified from their distinct backscattering signatures. Finer-grained deposits like lahars and pyroclastic density currents were not distinguishable by

backscatter alone. Coupling backscatter data with surface roughness estimates made from the ALS allowed for differentiation of lahar and debris avalanche deposits.

Among some of the earliest RS based vegetation studies in the BZ, Harrington et al. (1998) used Landsat Multi-Spectral Scanner (MSS) data from 1979, 1980, and even years through 1992 to study vegetation changes at MSH. All data were from summertime dates to ensure good vegetation data and minimize snow cover issues. The data were converted to NDVI reflectance values and georeferenced for time series analysis. By 1992, Harrington et al. (1998) found that vegetation growth was visible, particularly in replanted areas. Areas replanted by WEYCO showed the greatest increase in NDVI values. The study highlighted that timing of replanting, species planted, and ash removal influenced recovery.

Lawrence and Ripple (1998) analyzed the revegetation of Mount St. Helens using Landsat images. The study area consisted of the NVM and portions of GPNF. Ground visits in the summer of 1996 aided in image interpretation. For each sample, the average reflectance values for various vegetation indices were computed. Among the seven indices tested, NDVI performed the best.

Lawrence and Ripple (2000) used eight dates of Landsat images to estimate change curves representing the trajectories of green vegetation cover. Explanatory variables, such as disturbance type, blast exposure, distance from surviving forests, slope gradient, slope curvature, and aspect, were gathered in the field and input into a GIS. Their analysis showed that disturbance mechanisms, intensity of disturbances, distance from surviving forests, erosion on steeper slopes, and aspect significantly influenced early revegetation patterns.

Marzen et al. (2011) utilized ten Landsat images to analyze vegetation changes over time at MSH. Cloud-free images from the months of July or August were used to ensure consistent comparisons with minimal snow cover. NDVI was employed to estimate vegetation conditions. Precipitation data and scaled NDVI for the BZ were included in the analysis. Field trips in 1999 and 2000, along with ground photography visits, provided valuable insights for image interpretation. The study area consisted of the entire BZ and the properties within it. The analysis showed that average NDVI values increased the most following the 1980 eruption until 1992 and then stabilized. WEYCO lands had the highest average NDVI values, followed by WDNR, GPNF, and the NVM, which had the lowest NDVI values. Factors such as elevation, recent clear-cuts, and management approaches were believed to have influenced the differences in NDVI values (Figure 2.6).

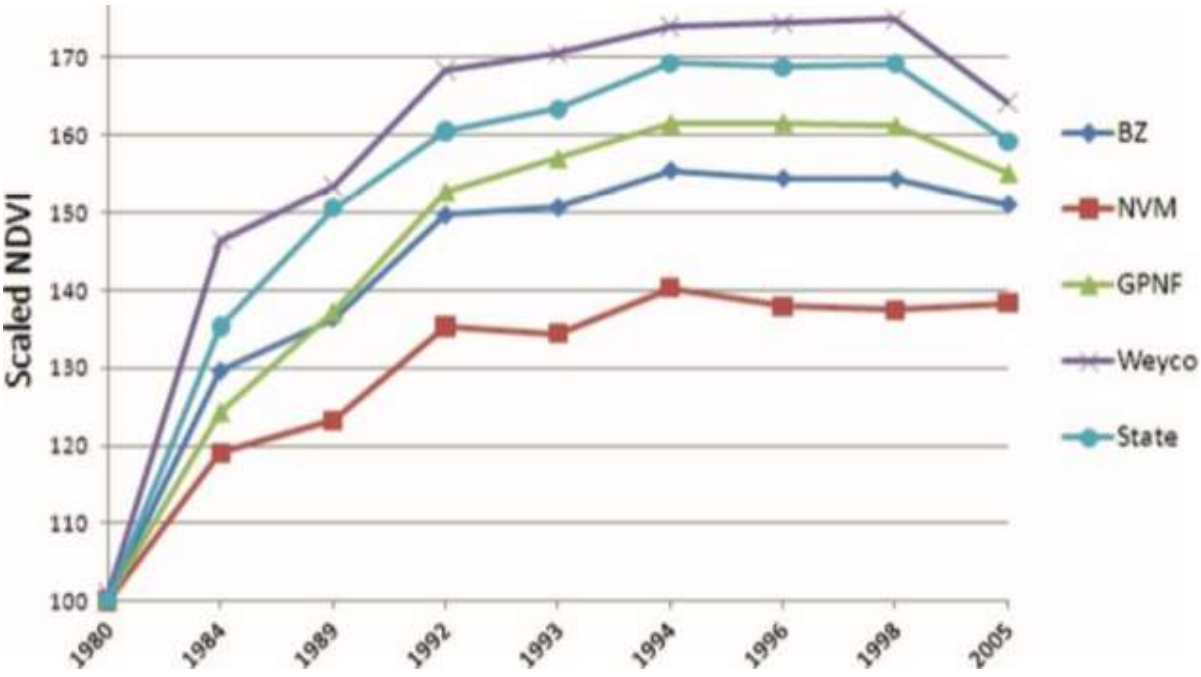

Figure 2.6: Scaled NDVI values from 1980 – 2005. The "Weyco" data was taken from managed timberland. The "NVM" data was taken from some of the least managed public property. From Marzen et al. (2011)

Li (2022) used images from the Landsat Collection 2 level 2 dataset, which includes improved atmospheric corrections for more accurate results. The study employed the NDVI to assess vegetation cover, using thresholds of 0.2 and 0.5 to distinguish between non-vegetated and fully vegetated areas. NDVI values were calculated and reclassified using a GIS called QGIS. Vegetated ground fluctuated significantly from 2009 to 2019, and there was a rebound in non-vegetated ground in 2014.

Teltscher and Fassnacht (2018) Used Five Landsat images from the years 1984, 1994, 2004, 2014, and 2016. Additionally, Sentinel-2 images, available since 2015 with higher spatial and spectral resolution, were applied to achieve more accurate land-cover classification. Change Vector Analysis was conducted to identify changes in vegetation cover over time, using NDVI. Supervised classification was performed using Sentinel-2 images to map the current land-cover, and numerical validation was carried out to determine accuracy. Regrowth started at the edges of the devastated area and moved closer to the volcano over time. From 1984 to 1994, approximately 462 km^2 were revegetated, while new vegetation losses covered 54 km^2.

2.8 References

Al-Wassai, F. A., & Kalyankar, N. V. (2013). *Major limitations of satellite images*. arXiv.org. https://arxiv.org/abs/1307.2434

Austin, S. A. (1986). *Mount St. Helens and catastrophism*. Mount St. Helens and Catastrophism. https://www.icr.org/article/mount-st-helens-catastrophism

Azuma , D., Christensen, G., Donnegan, J., Fried, J., Weyermann, D., Monleon, V., Kueglar, O., & Jovan, S. (2006). *Washington's Forest Resources, - 2002–2006*. U.S. Forest Service. https://www.fs.usda.gov/pnw/pubs/pnw_gtr800.pdf

Bannari, A., Morin, D., Bonn, F., & Huete, A. R. (1995). A review of vegetation indices. *Remote Sensing Reviews*, *13*(1–2), 95–120. https://doi.org/10.1080/02757259509532298

Binkley, C. S. (2005). The environmental benefits of tree plantations. *Journal of Sustainable Forestry*, *21*(4), 5–14. https://doi.org/10.1300/j091v21n04_02

Chen, S., Wu, S., & Yang, J. (2025). Forest Management has a mixed effect on understory biomass, but understory species diversity and stand structure are key. *European Journal of Forest Research*. https://doi.org/10.1007/s10342-024-01753-2

Cook, J. E., & Halpern, C. B. (2018). Vegetation changes in blown-down and scorched forests 10–26 years after the eruption of Mount St. Helens, Washington, USA. *Plant Ecology*, *219*(8), 957–972. https://doi.org/10.1007/s11258-018-0849-8

Cracknell, A. P. (2018). The development of remote sensing in the last 40 years. *International Journal of Remote Sensing*, *39*(23), 8387–8427. https://doi.org/10.1080/01431161.2018.1550919

Dale, V. H., & Crisafulli, C. M. (2018). Ecological responses to the 1980 eruption of Mount St. Helens: Key lessons and remaining questions. *Ecological Responses at Mount St. Helens: Revisited 35 Years after the 1980 Eruption*, 1–18. https://doi.org/10.1007/978-1-4939- 7451-1_1

Dale, V. H., Swanson, F. J., & Crisafulli, C. M. (2005). Ecological Perspectives on management of the mount st. helens landscape. *Ecological Responses to the 1980 Eruption of Mount St. Helens*, 277–286. https://doi.org/10.1007/0-387-28150-9_19

Davis, R. W., Bender, L. C., Mausel, P. W., Chapa-Vargas, L., & Warner, R. E. (2010). Modeling post-eruption habitat changes for deer at Mount St. Helens using remote sensing and GIS. *Geospatial Technologies in Environmental Management*, 11–28. https://doi.org/10.1007/978-90-481-9525-1_2

Decker, R., & Decker, B. (1981). The Eruptions of Mount St. Helens. *Scientific American*, *244*(3), 68–81. http://www.jstor.org/stable/24964328

Denny, E. G., Gerst, K. L., Miller-Rushing, A. J., Tierney, G. L., Crimmins, T. M., Enquist, C. A., Guertin, P., Rosemartin, A. H., Schwartz, M. D., Thomas, K. A., & Weltzin, J. F. (2014). Standardized phenology monitoring methods to track plant and animal activity for Science and Resource Management Applications. *International Journal of Biometeorology*, *58*(4), 591–601. https://doi.org/10.1007/s00484-014-0789-5

Efremenko, D., & Kokhanovsky, A. (2021). Introduction to remote sensing. *Foundations of Atmospheric Remote Sensing*, 1–35. https://doi.org/10.1007/978-3-030-66745-0_1

Frank, D., Meier, M. F., Swanson, D. A., with contributions by Babcock, J. W., Fretwell, M. O., Malone, S. D., Rosenfeld, C. L., Shreve, R. L., & Wilcox, R. E. (1977). Assessment of increased thermal activity at Mount Baker, Washington, March 1975-March 1976.
Professional Paper. https://doi.org/10.3133/pp1022a

Franklin, J. F. (1990). Biological legacies: a critical management concept from Mt. St. Helens. In: McCabe, Richard E., ed. Transactions of the Fifty-fifth North American Wildlife and Natural Resources Conference ; 1990 March 16-21; Denver, CO. 55. Washington, DC: Wildlife Management Institute: 216-219.

Franklin, J. F., Frenzen, P. M., Swanson, F. J. (1988). Re-creation of ecosystems at Mount St. Helens: contrasts in artificial and natural approaches. In: Cairns, John Jr., ed. Rehabilitating damaged ecosystems. Boca Raton, FL: CRC Press, Inc.: 2: 1-37.

Halpern, C. B., Frenzen, P. M., Means, J. E., & Franklin, J. F. (1990). Plant Succession in Areas of Scorched and Blown-Down Forest after the 1980 Eruption of Mount St. Helens, Washington. *Journal of Vegetation Science*, *1*(2), 181–194. https://doi.org/10.2307/3235657

Harrington, L. M. B., Harrington, J. A., & Frenzen, P. M. (1998). Vegetation change in the mount st. helens (U.S.A.) Blast Zone, 1979–1992. *Geocarto International*, *13*(1), 75–82. https://doi.org/10.1080/10106049809354631

Huang, S., Tang, L., Hupy, J. P., Wang, Y., & Shao, G. (2020). A commentary review on the use of Normalized Difference Vegetation Index (NDVI) in the era of popular remote sensing. *Journal of Forestry Research*, *32*(1), 1–6. https://doi.org/10.1007/s11676-020-01155-1

Jelinski, D. E., & Wu, J. (1996). The modifiable areal unit problem and implications for landscape ecology. *Landscape Ecology*, *11*(3), 129–140. https://doi.org/10.1007/bf02447512

Kerr, J. T., & Ostrovsky, M. (2003). From space to species: Ecological applications for remote sensing. *Trends in Ecology & Evolution*, *18*(6), 299–305. https://doi.org/10.1016/s0169-5347(03)00071-5

Lawrence, R. (2005). Remote Sensing of Vegetation Responses During the First 20 Years Following the 1980 Eruption of Mount St. Helens: A Spatially and Temporally Stratified Analysis. In: Dale, V.H., Swanson, F.J., Crisafulli, C.M. (eds) Ecological Responses to the 1980 Eruption of Mount St. Helens. Springer, New York, NY. https://doi.org/10.1007/0-387-28150-9_8

Lawrence, Rick & Ripple, William. (2000). Fifteen Years of Revegetation of Mount St. Helens: A Landscape-Scale Analysis. Ecology. 81. 10.2307/177338.

Lawrence, R. L., & Ripple, W. J. (1998). Comparisons among vegetation indices and bandwise regression in a highly disturbed, heterogeneous landscape: Mount St. Helens, Washington. *Remote Sensing of Environment*, *64*(1), 91–102. https://doi.org/10.1016/s0034- 4257(97)00171-5

Li, Z. (2022). Spatial distribution and temporal change of vegetation restoration after the eruption of Mount St. Helens: From 1984 to 2019. *Highlights in Science, Engineering and Technology*, *17*, 133–141. https://doi.org/10.54097/hset.v17i.2555

Liu, C. L., Kuchma, O., & Krutovsky, K. V. (2018). Mixed-species versus monocultures in plantation forestry: Development, benefits, ecosystem services and perspectives for the future. *Global Ecology and Conservation*, *15*. https://doi.org/10.1016/j.gecco.2018.e00419

Lovett, R. A. (2000). Mount St. Helens, revisited. *Science*, *288*(5471), 1578–1579. https://doi.org/10.1126/science.288.5471.1578

Markham, K., Frazier, A. E., Singh, K. K., & Madden, M. (2022). A review of methods for scaling remotely sensed data for spatial pattern analysis. *Landscape Ecology*, *38*(3), 619–635. https://doi.org/10.1007/s10980-022-01449-1

Marzen, L. J., Szantoi, Z., Harrington, L. M. B., & Harrington, J. A. (2011). Implications of management strategies and vegetation change in the mount st. helens blast zone. *Geocarto International*, *26*(5), 359–376. https://doi.org/10.1080/10106049.2011.584977

Miller, C. D. (1990). Volcanic Hazards in the Pacific Northwest. *Geoscience Canada*, *17*(3). Retrieved from https://journals.lib.unb.ca/index.php/GC/article/view/3676

Mierzejowska, A., & Żogała, M. (2018). The characteristics of geographical information systems in terms of their current use. *Journal of Water and Land Development*, *39*(1), 101–108. https://doi.org/10.2478/jwld-2018-0064

Moral, R. del, & Wood, D. M. (1993). Early primary succession on the volcano Mount St. Helens. *Journal of Vegetation Science*, *4*(2), 223–234. https://doi.org/10.2307/3236108

Moral, R. del, Walker, L. R., & Bakker, J. P. (2007). Insights gained from succession for the restoration of landscape structure and function. *SPRINGER SERIES ON ENVIRONMENTAL MANAGEMENT*, 19–44. https://doi.org/10.1007/978-0-387-35303-6_2

Mount St. Helens - 40 years after the blast. Washington Trails Association. (n.d.). https://www.wta.org/news/magazine/features/mount-st-helens-2014-40-years-after-the- blast

Nash, S. (2010). Making sense of mount st. helens. *BioScience*, *60*(8), 571–575. https://doi.org/10.1525/bio.2010.60.8.3

National Research Council. (1994). *Mount Rainier: Active Cascade Volcano*. Washington, DC: The National Academies Press. https://doi.org/10.17226/4546.

Oh, S., Jung, J., Shao, G., Shao, G., Gallion, J., & Fei, S. (2022). High-resolution canopy height model generation and validation using USGS 3DEP Lidar Data in Indiana, USA. *Remote Sensing*, *14*(4), 935. https://doi.org/10.3390/rs14040935

Parece, T. E., & Campbell, J. B. (2015). Land use/land cover monitoring and Geospatial Technologies: An overview. *The Handbook of Environmental Chemistry*, 1–32. https://doi.org/10.1007/978-3-319-14212-8_1

Peng, D., Wu, C., Li, C., Zhang, X., Liu, Z., Ye, H., Luo, S., Liu, X., Hu, Y., & Fang, B. (2017). Spring Green-up Phenology Products derived from Modis Ndvi and evi: Intercomparison, interpretation and validation using National Phenology Network and Ameriflux Observations. *Ecological Indicators*, *77*, 323–336. https://doi.org/10.1016/j.ecolind.2017.02.024

Pirard, R., Dal Secco, L., & Warman, R. (2016). Do timber plantations contribute to forest conservation? *Environmental Science & Policy*, *57*, 122–130. https://doi.org/10.1016/j.envsci.2015.12.010
Pricope, N. G., & Bashit, M. S. (2023). Emerging trends in topobathymetric Lidar Technology and mapping. *International Journal of Remote Sensing*, *44*(24), 7706–7731. https://doi.org/10.1080/01431161.2023.2287564
Racine, E. B., Coops, N. C., Bégin, J., & Myllymäki, M. (2021). Tree species, crown cover, and age as determinants of the vertical distribution of Airborne Lidar returns. *Trees*, *35*(6), 1845–1861. https://doi.org/10.1007/s00468-021-02155-2
Racine, E. B., Coops, N. C., St-Onge, B., & Bégin, J. (2014). Estimating forest stand age from Lidar-derived predictors and nearest neighbor imputation. *Forest Science*, *60*(1), 128–136. https://doi.org/10.5849/forsci.12-088
Robbins, W. G. (1985). The social context of forestry: The Pacific Northwest in the Twentieth Century. *The Western Historical Quarterly*, *16*(4), 413. https://doi.org/10.2307/968606
Rochelle, J. A., Ford, R. L., & Terry, T. A. (1992). The Reforestation Challenge. *Journal of Forestry*, *90*(5), 20–24. https://doi.org/10.1093/jof/90.5.20
Rogic, N., Charbonnier, S. J., Garin, F., Dayhoff II, G. W., Gagliano, E., Rodgers, M., Connor, C. B., Varma, S., & Shean, D. (2023). Characterizing and mapping volcanic flow deposits on Mount St. Helens via dual-band sar imagery. *Remote Sensing*, *15*(11), 2791. https://doi.org/10.3390/rs15112791
Snellgrove, T. A., Kendall Snell, J. A., & Max, T. A. (1983). Damage to national forest timber on Mount St. Helens. *Journal of Forestry*, *81*(6), 368–371. https://doi.org/10.1093/jof/81.6.368
Teltscher, K., & Fassnacht, F. E. (2018). Using multispectral landsat and sentinel-2 satellite data to investigate vegetation change at Mount St. Helens since the Great Volcanic eruption in 1980. *Journal of Mountain Science*, *15*(9), 1851–1867. https://doi.org/10.1007/s11629-018-4869-6
Titus, J. H., & Householder, E. (2007). Salvage logging and replanting reduce understory cover and richness compared to unsalvaged-unplanted sites at Mount St. Helens, Washington. *Western North American Naturalist*, *67*(2), 219–231. https://doi.org/10.3398/1527-0904(2007)67[219:slarru]2.0.co;2
USDA Natural Resources Conservation Service. *Forest Management and Forest Stand Improvement*. (2023). https://www.nrcs.usda.gov/sites/default/files/2024-01/Forest%20Stand%20Improvement%20FS-SD-123.pdf
USGS. (2024). *Landsat missions timeline*. USGS. https://www.usgs.gov/media/images/landsat-missions-timeline
USGS. (2023). *Newest Volcano Notice Including Mount St. Helens*. Newest volcano notice including Mount St. Helens. https://volcanoes.usgs.gov/hans-public/volcano/wa4
USGS. (2023). *The 2004-2008 eruption of Mount St. Helens and "what ifs."* USGS. https://www.usgs.gov/volcanoes/mount-st.-helens/science/2004-2008-eruption-mount-st-helens-and-what-ifs?form=MG0AV3
USGS. (2023). *Earthquake monitoring at Mount St. Helens*. USGS. https://www.usgs.gov/volcanoes/mount-st.-helens/science/earthquake-monitoring-mount-st-helens?form=MG0AV3

USGS. (1981). *The 1980 Eruptions of Mount St. Helens, Washington*. MSH lateral "blast" [USGS]. https://pubs.usgs.gov/gip/msh/lateral.html

Vaughan, R. G., Hook, S. J., Ramsey, M. S., Realmuto, V. J., & Schneider, D. J. (2005). Monitoring eruptive activity at Mount St. Helens with Tir Image Data. *Geophysical Research Letters*, *32*(19). https://doi.org/10.1029/2005gl024112

Wang, X., Pan, H., Guo, K., Yang, X., & Luo, S. (2020). The evolution of LIDAR and its application in high precision measurement. *IOP Conference Series: Earth and Environmental Science*, *502*(1), 012008. https://doi.org/10.1088/1755-1315/502/1/012008

Wang, K., Franklin, S. E., Guo, X., & Cattet, M. (2010). Remote Sensing of ecology, Biodiversity and Conservation: A review from the perspective of remote sensing specialists. *Sensors*, *10*(11), 9647–9667. https://doi.org/10.3390/s101109647

Waring, R. H., & Franklin, J. F. (1979). Evergreen coniferous forests of the Pacific Northwest. *Science*, *204*(4400), 1380–1386. https://doi.org/10.1126/science.204.4400.1380

WDNR. (2017). *Landslides of mount st. helens activity book*. dnr.wa.gov. https://www.dnr.wa.gov/publications/ger_landslide_activity_book.pdf

Wehr, A., & Lohr, U. (1999). Airborne Laser Scanning—an introduction and Overview. *ISPRS Journal of Photogrammetry and Remote Sensing*, *54*(2–3), 68–82. https://doi.org/10.1016/s0924-2716(99)00011-8

Winjum, J. K., Keatley, J. E., Stevens, R. G., & Gutzwiler, J. R. (1986). Regenerating the blast zone of Mount St. Helens. *Journal of Forestry*, *84*(5), 28–35. https://doi.org/10.1093/jof/84.5.28

Wright, H. M., Driedger, C. L., Pallister, J. S., Newhall, C. G., Clynne, M. A., & Ewert, J. W. (2023). Development of a volcanic risk management system at Mount St. helens—1980 to present. *Bulletin of Volcanology*, *85*(10). https://doi.org/10.1007/s00445-023-01663-y

Chapter 3: Vegetation Re-establishment at MSH Between 1984 and 2024

3.0 Introduction

Forests are well known for the products and services they supply. Forests provide essential ecosystem services such as controlling carbon, soil erosion, and air quality. Exceptional levels of carbon are stored in the forests of the Pacific Northwest which makes them important for controlling the terrestrial carbon sink (Krankina et al., 2014). They also contribute to the global GDP by providing lumber, paper, and other related products (Wardle & Kaoneka, 1999). Because of the important role they play across multiple fronts, forests must be monitored and protected. With increasing natural and human caused threats to forests, the implementation of sustainable forest management has become crucial. In response to environmental concerns, government agencies have even developed programs to monitor forest health (Lausch et al., 2016). One program, The Forest Health Monitoring Program (FHM) was established by the U.S. Forest Service. The FHM program was a national initiative which was created to assess current forest conditions. The program utilizes data from ground surveys, Remote Sensing (RS), and other sources to evaluate forest health and the sustainability of forests and their related ecosystems (U.S. Forest Service, n.d.). The system encourages the use of RS for monitoring earth's forests.

Satellite based multispectral imagery is a method of RS which provides a comprehensive view of the environment, so it can capture information about forests and their relationships to each other at the landscape scale. Satellite RS has provided valuable information on forests, and ecologists have begun to use satellite data to monitor forest stands relying on the spectral characteristics without having to integrate information from

field studies (Shaw & Burke, 2003). Today, multispectral satellite imagery is available worldwide at different spatial and temporal scales. Multispectral sensors identify objects based on their spectral characteristics, which include specific reflectance or emission in portions of electromagnetic radiation (Navalgund et al., 2007). The USGS Landsat program is the longest continuous program of publicly available multispectral imagery and has provided imagery for most of the planet since 1972. Because imagery from Landsat is acquired under consistent parameters, there has been a standard in landscape scale measurements for over half a century. Satellite imagery is also a relatively inexpensive way to acquire data compared to field studies or even other methods of acquiring RS data such as UAS or airborne platforms (Lechner et al., 2020).

The use of satellite imagery to understand the ecological nature of forests is a rapidly evolving methodology. Though many forest monitoring RS applications are still experimental, Iverson et al., (1989) indicates that satellite imagery-based RS applications are valuable for extracting information about forest growth. The temporal resolution (nearly twice per month), data availability (free), and large footprint are the main benefits provided by Landsat imagery. In vegetation monitoring using multispectral data, the red and near-infrared bands are the most widely used wavelengths for producing vegetation indices (Xie et al., 2008). The Normalized Difference Vegetation Index (NDVI), a common vegetation index, is often used to monitor vegetation using optical RS platforms mounted on satellites. NDVI correlates with phenological activity such as leaf growth or expansion in vegetation and trees, and it provides quantitative measurements of such changes that occur (Prabakaran et al., 2013).

Spatiotemporal analysis of multispectral satellite imagery has been utilized in many other

studies where understanding re-establishment after natural or man-made disturbances occurred. Li et al. (2016) studied long term vegetation reestablishment around the city of New Orleans following Hurricane Katrina. Using NDVI, the authors conducted a spatiotemporal analysis of recovery of both urban vegetation and remote forests in. Lee & Chow (2015) used Landsat-derived NDVI to monitor vegetation reestablishment following wildfires in Texas. Monitoring the changes of the forests and vegetation following volcanic eruptions is important for understanding the reestablishment in blast zones (BZ) and especially at Mount St. Helens (MSH). Multiple previous studies at the MSH BZ have utilized NDVI to study the rate of growth of vegetation (Teltscher and Fassnacht, 2018, Marzen et al., 2011, Harrington et al., 1998, and Li, 2022), but no study has incorporated an Emerging Hot Spot Analysis (EHSA) tool on an annualized basis to assess the reestablishment patterns across the extended period of the years 1984 – 2024. The primary purpose of EHSA is to identify patterns and analyze the distribution of values across time and space. EHSA cannot be completed without a time series of data as the analysis uses time and spatial characteristics to draw conclusions (Abelairas-Etxebarria & Astorkiza, 2020). EHSA is a two-step process that first incorporates the Getis-Ord Gi* statistic (Ord and Getis, 1995) to assess the relationship of values such as NDVI values across space. The tool then uses the Mann – Kendall statistic (Mann, 1945) to test the relationship of the values across time. In the BZ this is significant as it enables the comparison of vegetation reestablishment patterns across the entire BZ or on separate properties.

3.1 Study Area

The study area of the MSH blast zone will be broken down based on the management areas described in Marzen et al. (2011). These management areas consist of Weyerhaeuser Company (WEYCO), Gifford Pinchot National Forest (GPNF), National Volcanic Monument (NVM), and Washington Department of Natural Resources (WDNR). It is important to think of these as separate management areas as these ownership properties are each managed for separate outcomes. GPNF and WDNR have similar management styles which are torn between management for timber harvest, management for recreation, and management for preservation (WDNR n.d., USFSa n.d.). By law human activity in the NVM was strictly limited and therefore vegetation reestablishment was allowed to occur naturally following the eruption. Whereas after meeting government mandated safety protocols, WEYCO did everything possible to assist in reestablishment of timberland because the company is obligated to manage a productive timber stand (Washington State Geoservices, 2024). Due to various management strategies of each property area EHSA will be completed on each of the separate management areas as separate zones within the BZ study area (Figure 3.0).

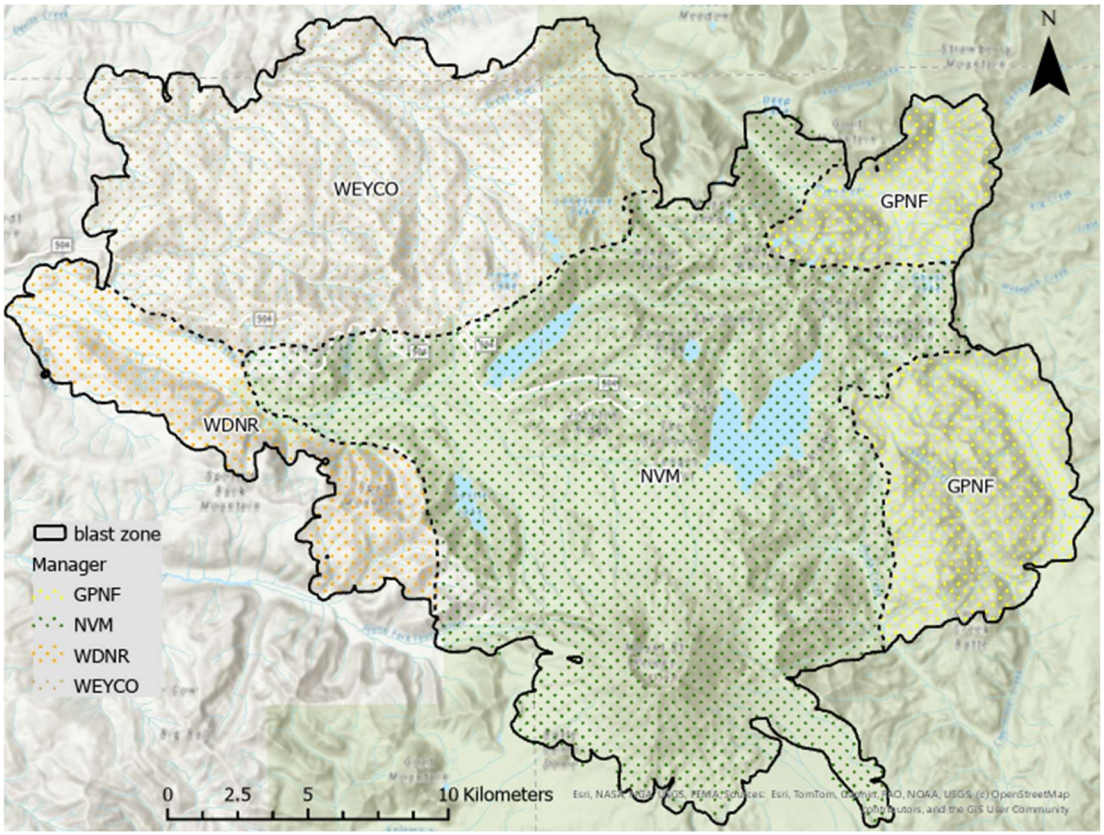

Figure 3.0: This is a map of the blast zone, and the different property managers that lie within it. Ownership information courtesy of Washington State Geoservices (2024).

3.2 Research Objective

The first objective of this study is to track the growth of vegetated and forested areas throughout the years 1984 – 2024 in the MSH BZ by utilizing EHSA of NDVI values to determine growth patterns that have occurred within the BZ.

Completing the research objective will answer the question:

Q1. How has vegetation been reestablished across time and space in the various management areas in the blast zone over the past 40 years?

3.3 Methods

3.3.1 Data

Landsat data (EROS, 2020) will be the main data component of this study. An anniversary series of Landsat images have been gathered each year from the summer of 1984 to the summer of 2024. While the eruption occurred in 1980, Snellgrove et al. (1983) indicates that salvage logging and the removal of woody debris was still ongoing in 1983 particularly in the GPNF. This delay was attributed to the requirement to conduct environmental assessments which were necessary to complete prior to any equipment being allowed on the property to remove material and salvage timber.

Landsat Level 2 Collection 2 products undergo a significant amount of post processing to correct for atmospheric, radiometric and topographic errors and therefore were the chosen data product for this study. The benefits include having a high geolocation accuracy as well as improved radiometric and atmospheric correction to ensure accuracy and consistency across data collected from the TM, ETM, and OLI sensors (Crawford et al., 2023). Atmospheric corrections are important to minimize error in measurements, and the atmospheric corrections for Level 2 Collection 2 products included the use of the Landsat Ecosystem Disturbance Adaptive Processing System (LEDAPS) and Surface Reflectance Code (LASRC) processing algorithms which convert the imagery pixel values to reflectance values and account for atmospheric errors (Zhou et al., 2023). Level 2 Collection 2 images have been used in many studies for studying vegetation including some of the latest studies in the BZ (Li, 2022, and Teltscher and Fassnacht, 2018). The Collection 2 Level 2 images are stated as being analysis ready data and received the stamp

of approval by the Committee on Earth Observation Satellites (CEOS) sensors (Crawford et al., 2023). The Level 2 Collection 2 products have a spatial resolution of 30 meters. Nelson et al. (2009) found that spatial resolutions greater than 30 meters introduce large standard errors of forest estimates.

The images chosen had 20% cloud cover or less, but post download, quality assessment bands included with Landsat Level 2 Collection 2 data were used to select cloud free images in the BZ. The only exception in image collection was a lack of a quality image for the year 2012. The images were taken from the summer months to minimize the amount of snow on the ground and capture the vegetation while it is in peak growing season. NDVI images were created using the NIR and Red bands gathered from the surface reflectance products. The NDVI images were clipped to the individual study areas, and masks were applied to water bodies in the study area such as Spirit Lake, Castle Lake, and Coldwater Lake as no surface trees will grow there. Additionally, the volcano was clipped to the tree line (4,800 ft) above which no trees will grow at Mount St. Helens (USFSb, n.d.). The Landsat Images from 1984 – 2024 used are listed in Table 3.0.

Table 3.0: Dates of Landsat Level 2 Collection 2 images used for analysis.

Sensor	Date	Spatial Resolution
Landsat 5 TM	8/04/1984	30 meter
Landsat 5 TM	6/20/1985	30 meter
Landsat 5 TM	8/26/1986	30 meter
Landsat 5 TM	8/29/1987	30 meter
Landsat 5 TM	8/31/1988	30 meter
Landsat 5 TM	8/18/1989	30 meter
Landsat 5 TM	7/20/1990	30 meter
Landsat 5 TM	7/07/1991	30 meter
Landsat 5 TM	8/26/1992	30 meter
Landsat 5 TM	8/29/1993	30 meter
Landsat 5 TM	7/31/1994	30 meter
Landsat 5 TM	8/03/1995	30 meter
Landsat 5 TM	8/21/1996	30 meter
Landsat 5 TM	7/23/1997	30 meter
Landsat 5 TM	8/271998	30 meter
Landsat 5 TM	7/29/1999	30 meter
Landsat 5 TM	8/16/2000	30 meter
Landsat 5 TM	7/02/2001	30 meter
Landsat 5 TM	8/22/2002	30 meter
Landsat 5 TM	8/25/2003	30 meter
Landsat 5 TM	8/11/2004	30 meter
Landsat 5 TM	8/14/2005	30 meter
Landsat 5 TM	7/16/2006	30 meter
Landsat 5 TM	7/03/2007	30 meter
Landsat 5 TM	8/22/2008	30 meter
Landsat 5 TM	7/24/2009	30 meter
Landsat 5 TM	8/12/2010	30 meter
Landsat 5 TM	7/30/2011	30 meter
Landsat 8 OLI	8/20/2013	30 meter
Landsat 8 OLI	8/07/2014	30 meter
Landsat 8 OLI	8/26/2015	30 meter
Landsat 8 OLI	8/28/2016	30 meter
Landsat 8 OLI	7/30/2017	30 meter
Landsat 8 OLI	8/18/2018	30 meter
Landsat 8 OLI	8/05/2019	30 meter
Landsat 8 OLI	8/23/2020	30 meter
Landsat 8 OLI	8/10/2021	30 meter
Landsat 8 OLI	8/29/2022	30 meter
Landsat 8 OLI	8/24/2023	30 meter
Landsat 8 OLI	8/26/2024	30 meter

3.3.2 Analysis

NDVI is a common vegetation index used for measuring phenology. It is used to determine the extent of tree leaf growth or plant growth in the spring as well as the loss of leaves or vegetation in the fall (Peng et al., 2017). NDVI was found useful for vegetation analysis once multispectral data became available and has been very important to study vegetation at the landscape scale directly following the eruption of 1980. The NDVI was used by Marzen et al. (2011), Lawrence and Ripple (1998), and Harrington et al. (1998) papers, for qualitative and quantitative analysis of vegetation health after the 1980 eruption. These studies chose anniversary dates for time series analysis. Choosing summer dates for every image allowed for the measurement of growth in each year without the issues of snow in winter months and inconsistent leaf loss or gain in the fall and spring months.

Wang et al. (2010) reviewed multiple remote sensing indices valuable to both spatial scientists and ecologists. In their discussion of vegetation indices, they point out that the NDVI has been used in multiple studies to great success. Huang et al. (2020) stated that "The Normalized Difference Vegetation Index (NDVI), one of the earliest remote sensing analytical products used to simplify the complexities of multi-spectral imagery, is now the most popular index used for vegetation assessment." NDVI derived from Landsat images is a valuable resource for measuring forest and vegetation health and is often used in combination with LiDAR for above ground biomass estimations. To improve accuracy of measuring forest health, it is suggested that an NDVI time-series of images provides better results than a single NDVI image. Optical imagery is more readily available and has a

higher temporal resolution than other RS methods (Zhu & Liu, 2015). The NDVI is calculated using Near InfraRed (NIR) and Red wavelengths (Figure 3.1).

$$NDVI = \frac{NIR - Red}{NIR + Red}$$

Figure 3.1: The equation for NDVI calculation. This calculation occurs on a cell-by-cell basis in an image converting cells in a multispectral image into an NDVI image which represents valuable information about forest health.

Healthy vegetation shows high reflectance values for the NIR spectrum, while also absorbing visible red light. Meaningful output values with respect to vegetation from NDVI typically range from 0 to 1.0.

The EHSA tool was utilized to determine spatiotemporal patterns in vegetation or forested areas in the MSH BZ. This is an analysis which considers time, space, and reflectance values for each pixel across the study area (Cuba et al., 2022). A space – time cube was created using a time – series NDVI raster which is the accumulation of the 40 years of Landsat Images. Each bin in the space – time cube represents a raster NDVI value. In the cube, the bin below represents the NDVI value for the previous year while the bins beside represent changes in the NDVI value across space (Figure 3.2).

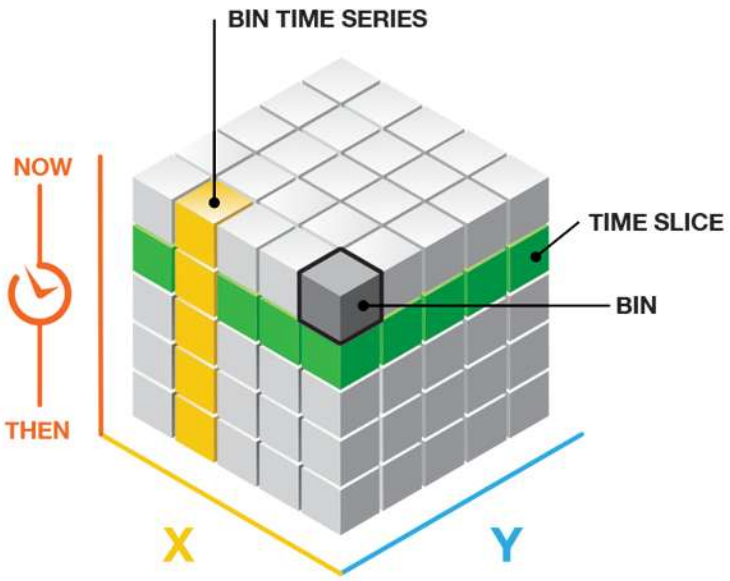

Figure 3.2. Conceptualization of Esri's space - time cube. From Esri a (n.d.).

Variation in NDVI is often discussed in terms of either temporal trends or spatial distribution. The differences between NDVI can be compared across a study area or between different time steps at one location. Xu et al. (2022) introduced the use of the space-time cube in their study of NDVI value changes over both space and time at the Jing River Basin of China. The choice of the EHSA method was due to the advantage of the analysis to consider trends across multiple time steps over time as well as spatial relationships of neighboring pixels. These relationships are then categorized based on two questions; (1) Is the pixel NDVI value significantly different than that of its spatially neighboring pixels; (2) Is the pixel NDVI value significantly changing when compared to its temporally neighboring pixels? Therefore, if there is a location with high NDVI values relative to its' neighbors then it is possible to determine whether this relationship is unique across multiple time steps. A pixel NDVI value may be higher than its spatial neighbors consistently across multiple time steps. It could have been higher than its neighbors across

the latest time steps, earliest time steps, or the single most recent time step. Therefore, this analysis considers the temporal trends and the spatial pattern of NDVI values over multiple time steps for a defined period.

The EHSA tool utilizes both the local and global Getis-Ord Gi* statistic (Ord and Getis, 1995) to determine the intensity of NDVI values in a bin relative to its neighboring bins across space. First, the significance of a bin's NDVI value difference is assessed relative to its neighboring bins using the local Getis-Ord Gi* statistic, and if it has a statistically significant Z score when compared to its neighborhood, the global Getis-Ord Gi* statistic compares the mean NDVI value of a bin's neighborhood to assess whether this bin is a cold or hot spot. Following the determination of whether a bin is a hot spot, cold spot, or not significant, the tool utilizes the Mann-Kendall trend test (Mann, 1945) to analyze trends across time. Across each time step, each bin's NDVI value is treated as an independent time series. Each year's NDVI value is compared to the previous year's. When compared to a previous bin, if the Z score of a bin is larger, then the result is an increasing trend. The Mann-Kendall trend test determines the temporal designation of a hot or cold spot. (Harris et al., 2017). Each time step for the space time cube will be 1 year, the bins of the space time cube will be the image pixel size of 30 meters, and the NDVI values of one bin will be compared to its' adjacent neighbors to determine the significance of a high or low value. These adjacent neighbors are defined as the edges and corners conceptualization of spatial neighbors often referred to as Queen conceptualization.

EHSA will classify values of each pixel based on the temporal trend and spatial clustering of NDVI values. The general categories produced in the Analysis consist of No Pattern, Hot Spot, and Cold Spot. For example, New Hot spot classifications represent a

pixel sized area with historically low NDVI values relative to the study area mean, but the most recent 2024 NDVI value has increased enough for this location to have an NDVI value higher than the study area mean (Devananda et al., 2024). Also, the NDVI values are becoming more intense over time. A Diminishing Cold Spot location represents an area which would have historically had low NDVI values, but the intensity of which this is a cold spot is lowering (Blachowski et al., 2023). There are a total of 17 potential classifications which are variations of hot and cold spot classifications (Figure 3.3).

	No Pattern Detected	Does not fall into any of the hot or cold spot patterns defined below.
	New Hot Spot	A location that is a statistically significant hot spot for the final time step and has never been a statistically significant hot spot before.
	Consecutive Hot Spot	A location with a single uninterrupted run of at least two statistically significant hot spot bins in the final time-step intervals. The location has never been a statistically significant hot spot prior to the final hot spot run and less than 90 percent of all bins are statistically significant hot spots.
	Intensifying Hot Spot	A location that has been a statistically significant hot spot for 90 percent of the time-step intervals, including the final time step. In addition, the intensity of clustering of high counts in each time step is increasing overall and that increase is statistically significant.
	Persistent Hot Spot	A location that has been a statistically significant hot spot for 90 percent of the time-step intervals with no discernible trend in the intensity of clustering over time.
	Diminishing Hot Spot	A location that has been a statistically significant hot spot for 90 percent of the time-step intervals, including the final time step. In addition, the intensity of clustering in each time step is decreasing overall and that decrease is statistically significant.

	Sporadic Hot Spot	A statistically significant hot spot for the final time-step interval with a history of also being an on-again and off-again hot spot. Less than 90 percent of the time-step intervals have been statistically significant hot spots and none of the time-step intervals have been statistically significant cold spots.
	Oscillating Hot Spot	A statistically significant hot spot for the final time-step interval that has a history of also being a statistically significant cold spot during a prior time step. Less than 90 percent of the time-step intervals have been statistically significant hot spots.
	Historical Hot Spot	The most recent time period is not hot, but at least 90 percent of the time-step intervals have been statistically significant hot spots.
	New Cold Spot	A location that is a statistically significant cold spot for the final time step and has never been a statistically significant cold spot before.
	Consecutive Cold Spot	A location with a single uninterrupted run of at least two statistically significant cold spot bins in the final time-step intervals. The location has never been a statistically significant cold spot prior to the final cold spot run and less than 90 percent of all bins are statistically significant cold spots.
	Intensifying Cold Spot	A location that has been a statistically significant cold spot for 90 percent of the time-step intervals, including the final time step. In addition, the intensity of clustering of low counts in each time step is increasing overall and that increase is statistically significant.
	Persistent Cold Spot	A location that has been a statistically significant cold spot for 90 percent of the time-step intervals with no discernible trend in the intensity of clustering of counts over time.
	Diminishing Cold Spot	A location that has been a statistically significant cold spot for 90 percent of the time-step intervals, including the final time step. In addition, the intensity of clustering of low counts in each time step is decreasing overall and that decrease is statistically significant.
	Sporadic Cold Spot	A statistically significant cold spot for the final time-step interval with a history of also being an on-again and off-again cold spot. Less than 90 percent of the time-step intervals have been statistically significant cold spots and none of the time-step intervals have been statistically significant hot spots.

	Oscillating Cold Spot	A statistically significant cold spot for the final time-step interval that has a history of also being a statistically significant hot spot during a prior time step. Less than 90 percent of the time-step intervals have been statistically significant cold spots.
	Historical Cold Spot	The most recent time period is not cold, but at least 90 percent of the time-step intervals have been statistically significant cold spots.

Figure 3.3. This figure displays the symbology of the EHSA output and explains what each pattern represents. From Esri b (n.d.).

3.4 Results

3.4.1 Initial NDVI Summary

The average NDVI values for all management areas have increased from 1984 to 2024. The average NDVI values in 1984, by property, were 0.44 (WEYCO), 0.36 (WDNR), 0.22 (GPNF), and 0.19 (NVM). There was a noticeable peak in 2006 where the properties reached average NDVI values of 0.85 (WEYCO), 0.77 (WDNR), 0.70 (GPNF), and 0.50 (NVM). Between the years 2006 – 2024, WEYCO dropped from an average NDVI value of 0.85 to 0.81 while the NVM average NDVI value rose from 0.50 to 0.65 between the years 2006 – 2024 (Figure 3.4).

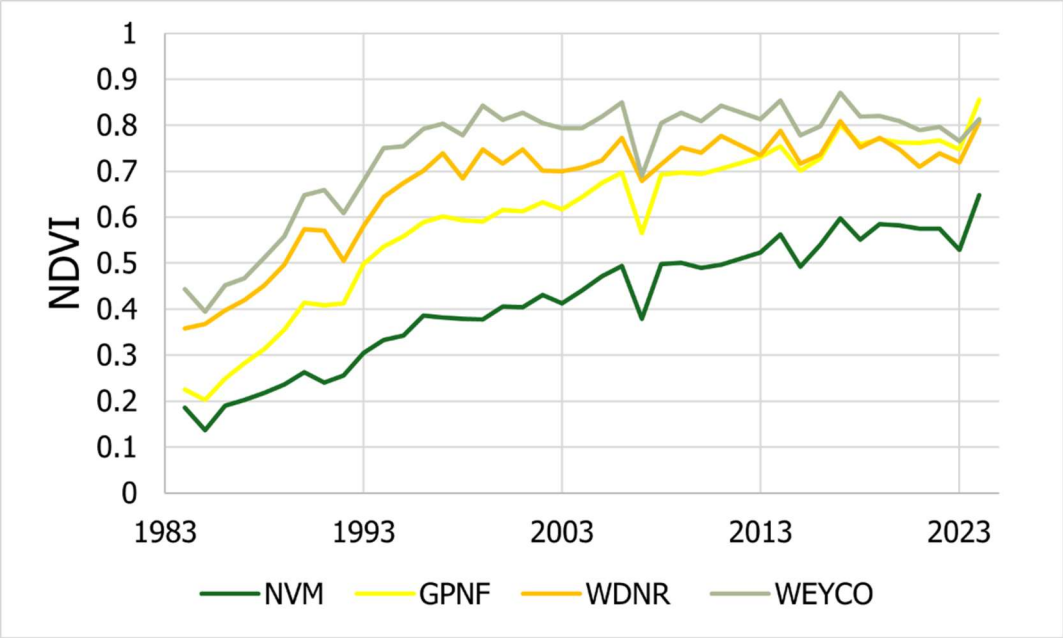

Figure 3.4. This figure represents the change in NDVI values across the different management areas between the years 1984 and 2024.

3.4.2 BZ EHSA Results

This study chose to analyze the extent and spatial pattern of vegetation reestablishment at MSH.. At first glance, the broad range of cold spot classifications are located on either the NVM management area closest to the volcano or in the North Toutle River valley which snakes it's way to the west from the NVM management area through the WDNR management area. (Figure 3.5).

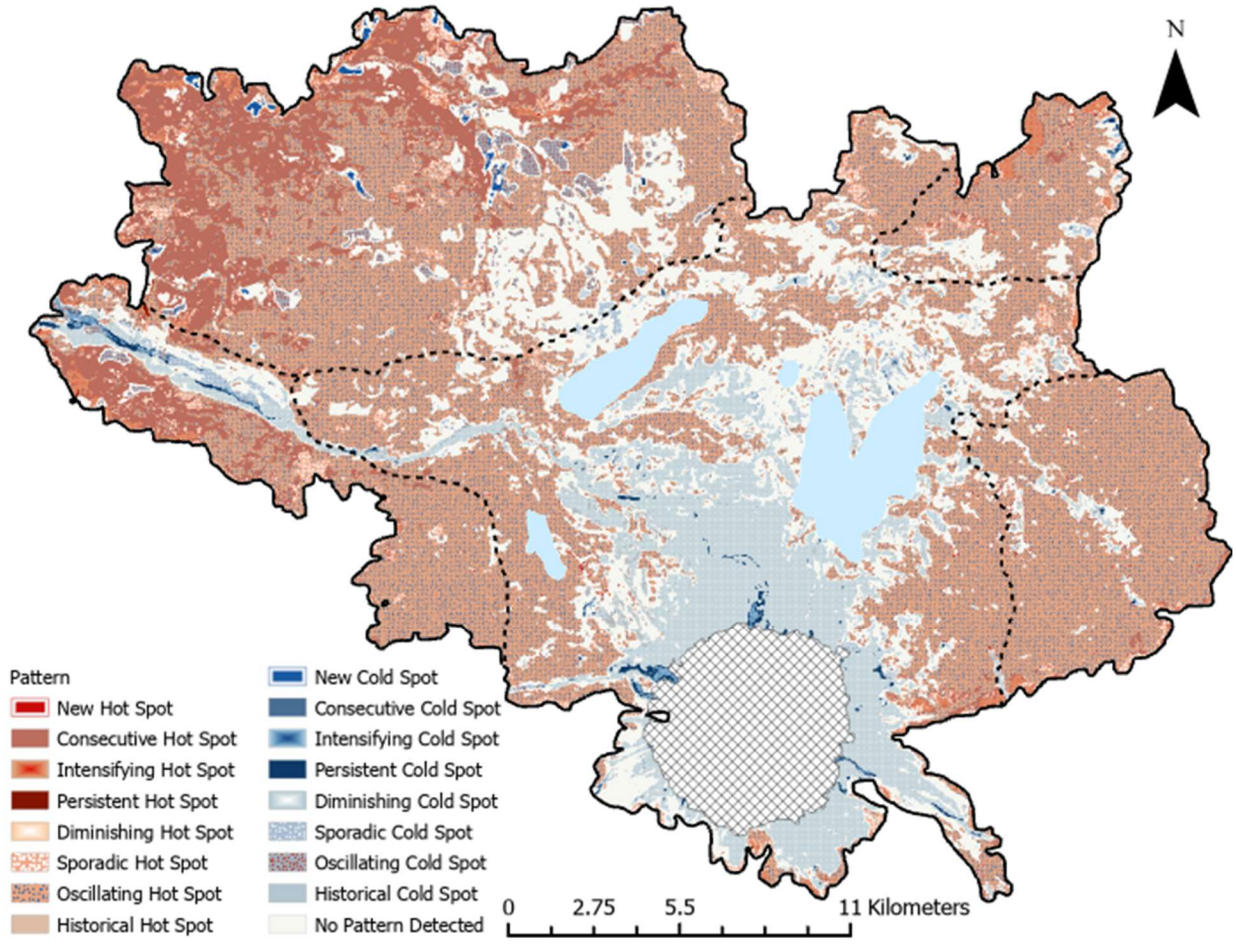

Figure 3.5. The output of EHSA of the BZ study area.

Of particular interest in the results are diminishing cold spots. (This pattern was a significant cold spot in atleast 90% of the images, including the final image, but the clustering of low NDVI pixels is decreasing over time) (Esri b, n.d.). These diminishing cold spots represent areas of NDVI which have historically been low, but the NDVI values have begun to increase in the latest time steps. Over 93% of the diminishing cold spots are in the NVM (Figure 3.6).

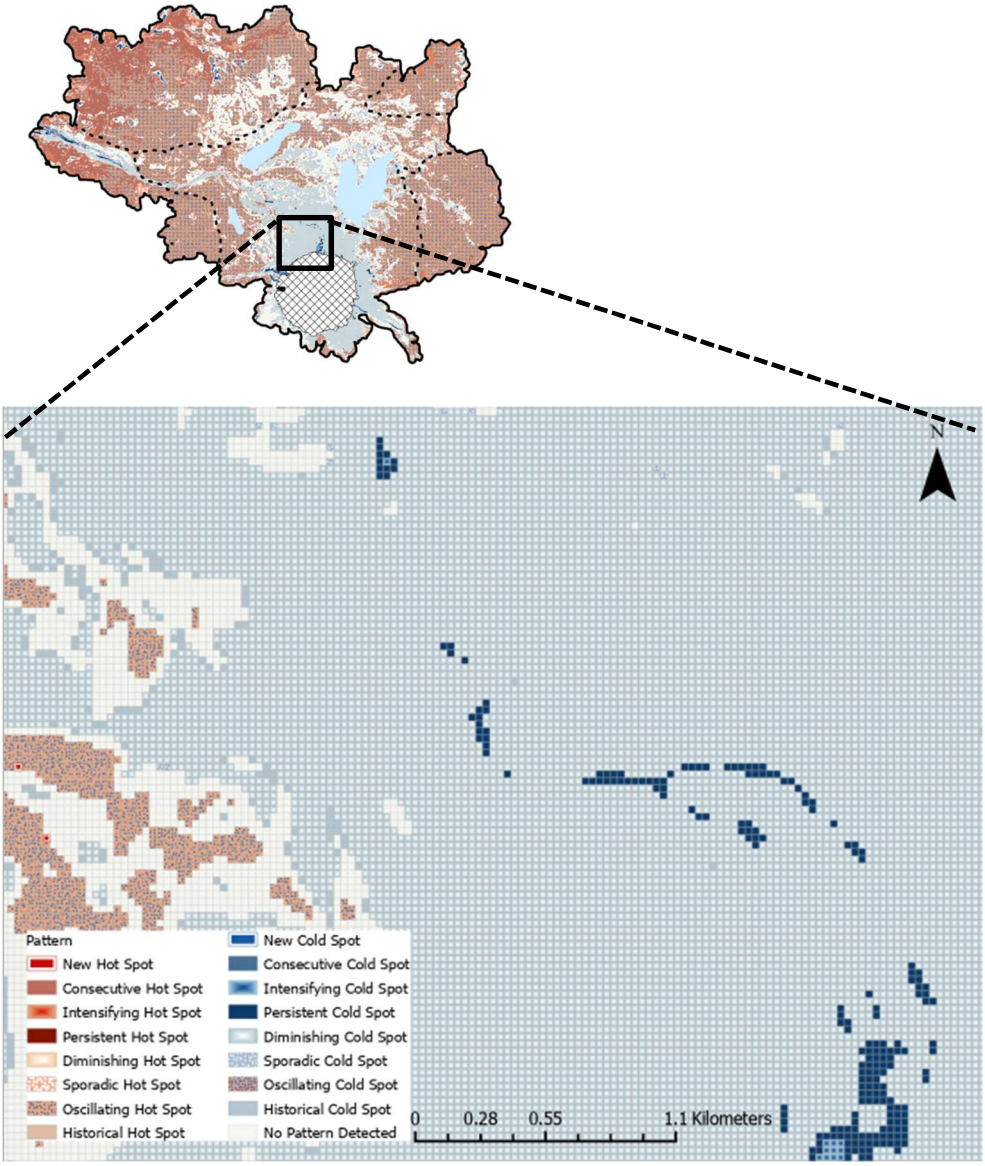

Figure 3.6. Diminishing cold spots of the NVM.

The initial analysis of the BZ showed that the WEYCO and WDNR management areas have some of the highest NDVI values which is validated by the assortment of hot spot classifications. The WEYCO management area has the most hot spots including persistent hot spots (a pixel that has been a hot spot in at least 90% of the images with no difference in the intensity of clustering of high NDVI pixels over time), historical hot spots (a pixel that is not a hot spot in the most recent image but has been a hot spot in at least 90% of the

previous images), consecutive hot spots (a pixel with a single uninterrupted run as a significant hot spot in the final time-step intervals while the pixel has never been a hot spot prior to the final hot spot run and is a hot spot in less than 90 % of the previous images), and intensifying hot spots (a pixel that has been a hot spot for at least 90% of the time-step intervals, including the final time step, with the clustering of surrounding high NDVI pixels in each image also increasing over time) (Esri b, n.d.) (Figure 3.7 and Table 3.1).

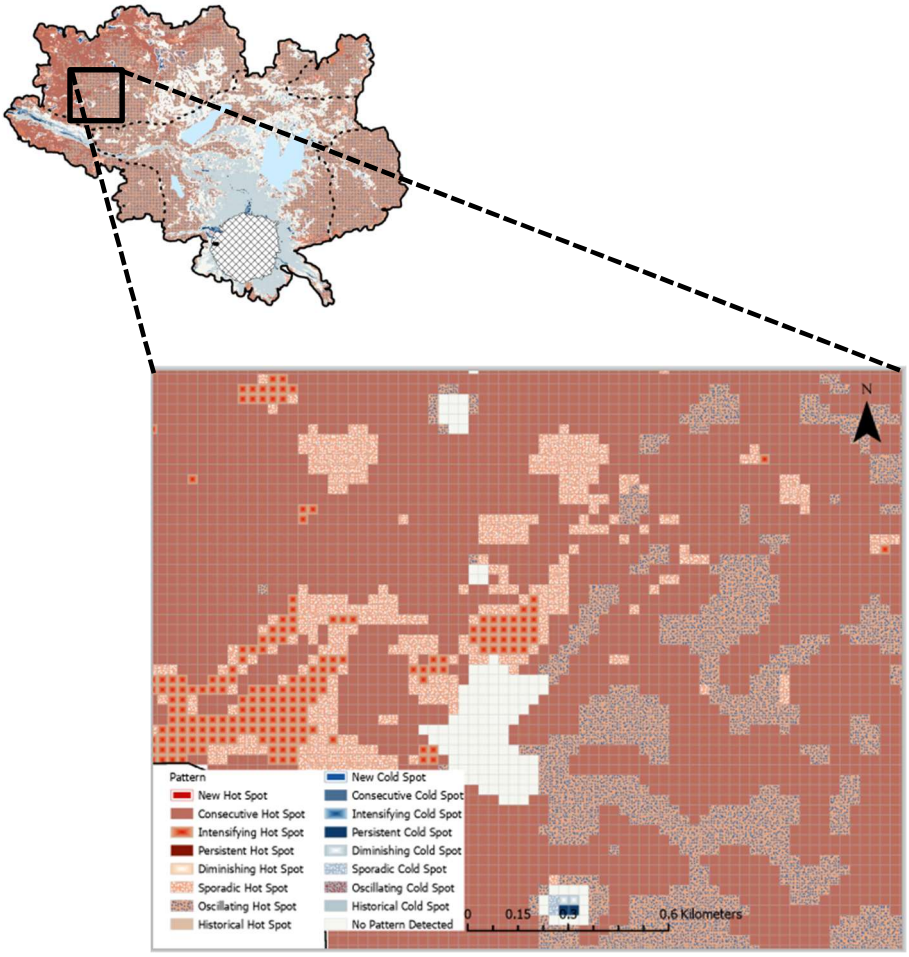

Figure 3.7. WEYCO hot spots.

Table 3.1. The following table lists the percentages of various hot and cold spot patterns recognized on the management areas during the analysis of the BZ.

	WEYCO	GPNF	NVM	WDNR
New Hotspot %	0.15	42.10	55.69	2.07
Diminishing Cold %	0.33	1.07	93.53	5.07
Oscillating Hot %	29.52	24.90	36.12	9.46
Persistent Hot %	39.40	0	3.46	57.14
Intensifying Hot %	41.03	27.09	13.97	17.91
Historical Hot %	95.12	0	0	4.88
Historical Cold %	0.25	6.78	90.49	2.48
Persistent Cold %	1.30	5.57	67.44	2.55
Consecutive Hot%	77.15	3.05	2.60	17.20

Of all the available patterns, the most common by far throughout the BZ is that of the oscillating hot spot which is a statistically significant hot spot for the final time-step interval that has a history of also being a statistically significant cold spot during prior time steps. Less than 90% of the time-step intervals have been statistically significant hot spots. Reviewing these areas in a cross section shows that the trend of these patterns are increasing NDVI values over time. The pixels underlying the oscillating hot spot began as low NDVI values making them cold spots and transitioned to hot spots of NDVI values in later years (Figure 3.8).

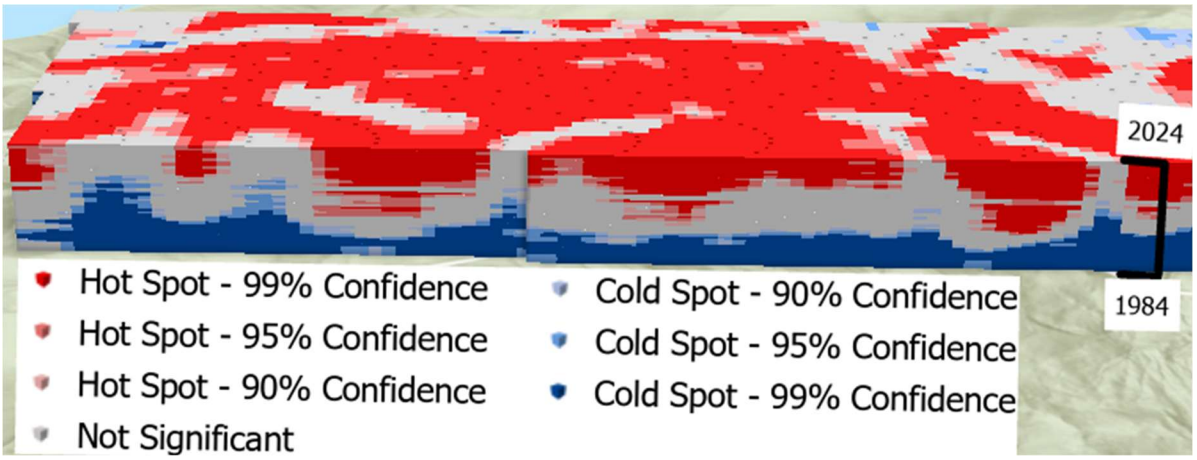

Figure 3.8. A cross section view of The NDVI space – time cube shows oscillating hot spots in the BZ where NDVI values have migrated from cold spots to hot spots over time.

3.4.3 Management Area EHSA Results

NVM Study Area

The EHSA of the NVM NDVI values shows that many of the cold spots close to the volcano are classified as diminishing cold spots. Areas with no pattern are also located close to the volcano where the NDVI values have not shown a significant enough trend to be determined a hot spot or cold spot. There are 35 km^2 of diminishing cold spots and new hot spots in the NVM management area. The diminishing cold spots and areas with no pattern are replaced with new hot spots (a pixel that is a hot spot for the final image and has never been a hot spot before) (Esri b, n.d.) and oscillating hot spots further to the northwest of the crater (Figure 3.9).

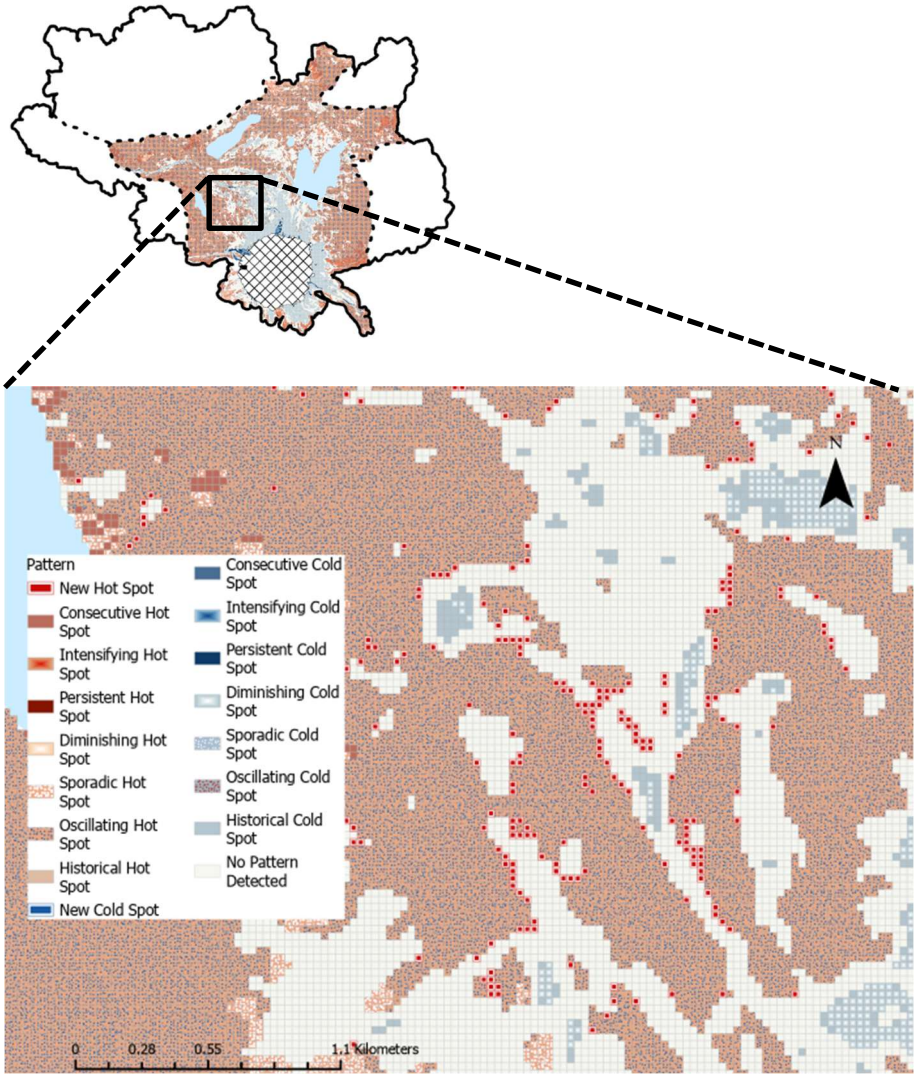

Figure 3.9. New hot spots and oscillating hot spots present in the output of the NVM EHSA.

Over 129 km^2 in the NVM are oscillating hotspots which are areas that began as cold spots and have become hotspots in later years. There are more oscillating hot spots than any other pattern in the NVM management area. Most importantly, there are no new cold spots (a pixel that is a cold spot in the final image and has never been a cold spot in previous images), but there are diminishing cold spots and persistent cold spots (a pixel that has been a cold spot in at least 90% of the images with no discernible trend in the

clustering of NDVI values over time) (Esri b, n.d.) located around drainage areas that descend from MSH such as the South Fork of the Toutle River and the Muddy River (Figure 3.10).

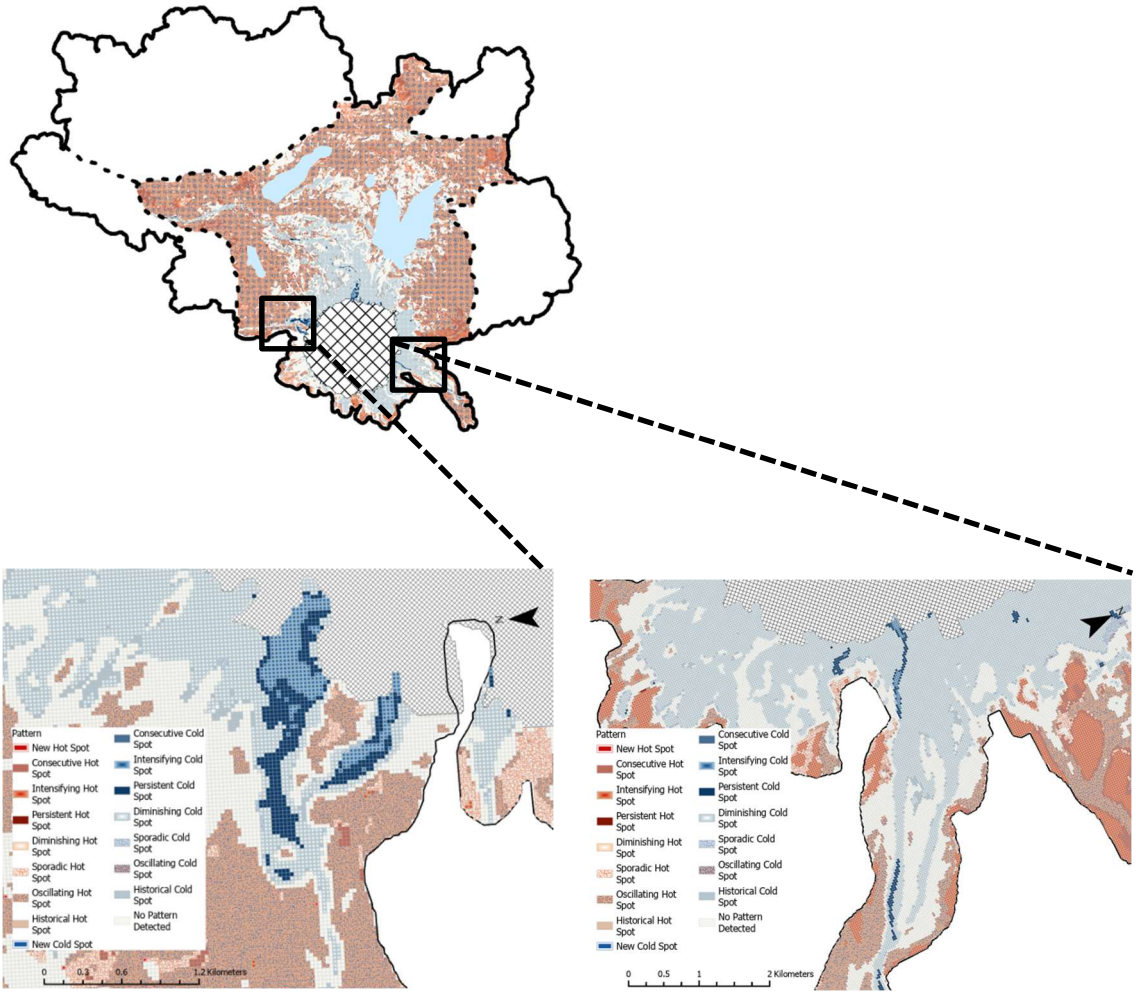

Figure 3.10. Cold spot patterns surrounding river valleys in the output of the NVM EHSA.

WDNR Study Area

The EHSA of WDNR found that cold spots of NDVI values lie in the lower elevations of the management area. Specifically, there was 5 km^2 of persistent cold spots (a pixel that has been a cold spot in at least 90% of the images with no discernible trend in the clustering of NDVI values over time), historical cold spots (the pixel in the most recent

image is not a cold spot, but at least 90% of the pixels in the previous images have been cold spots), and intensifying cold spots (a pixel that has been a cold spot in at least 90% of the images, including the final image, with the clustering of surrounding low NDVI values in each image also increasing) surrounding the North Fork of the Toutle River. There were no new cold spots (a pixel that is a cold spot in the final image and has never been a cold spot in previous images) (Esri b, n.d.), but the majority of the 1 km^2 of new hot spot classifications were located close to MSH on the Southeast corner of the WDNR management area (Figure 3.11).

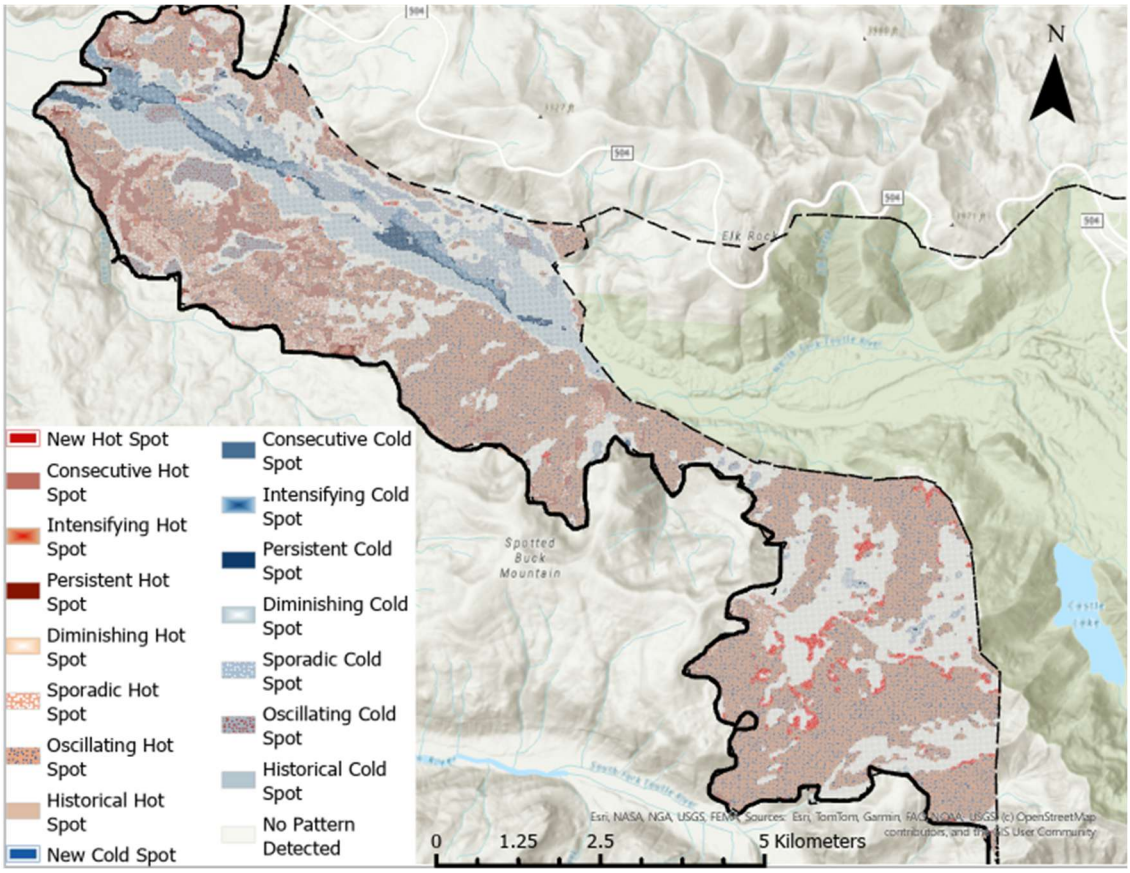

Figure 3.11. The output of the WDNR EHSA.

There are also 33 km^2 of oscillating cold spots on the WDNR management area (a pixel that is a cold spot in the final image that has a history of also being a hot spot in a prior image) (Esri b, n.d.). This makes these areas important to note as they are experiencing decreases of NDVI over time. The oscillating cold spots are in higher elevations above the North Fork of the Toutle River (Figure 3.12 and Figure 3.13).

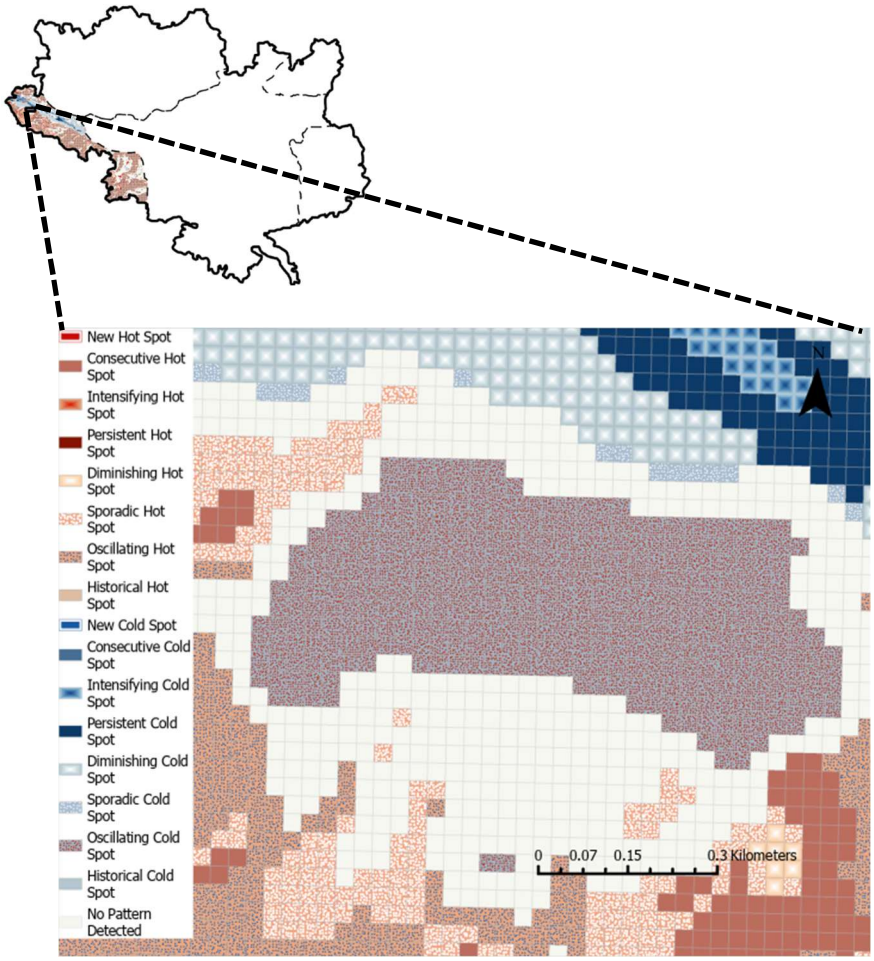

Figure 3.12. Oscillating cold spots present in the EHSA of WDNR.

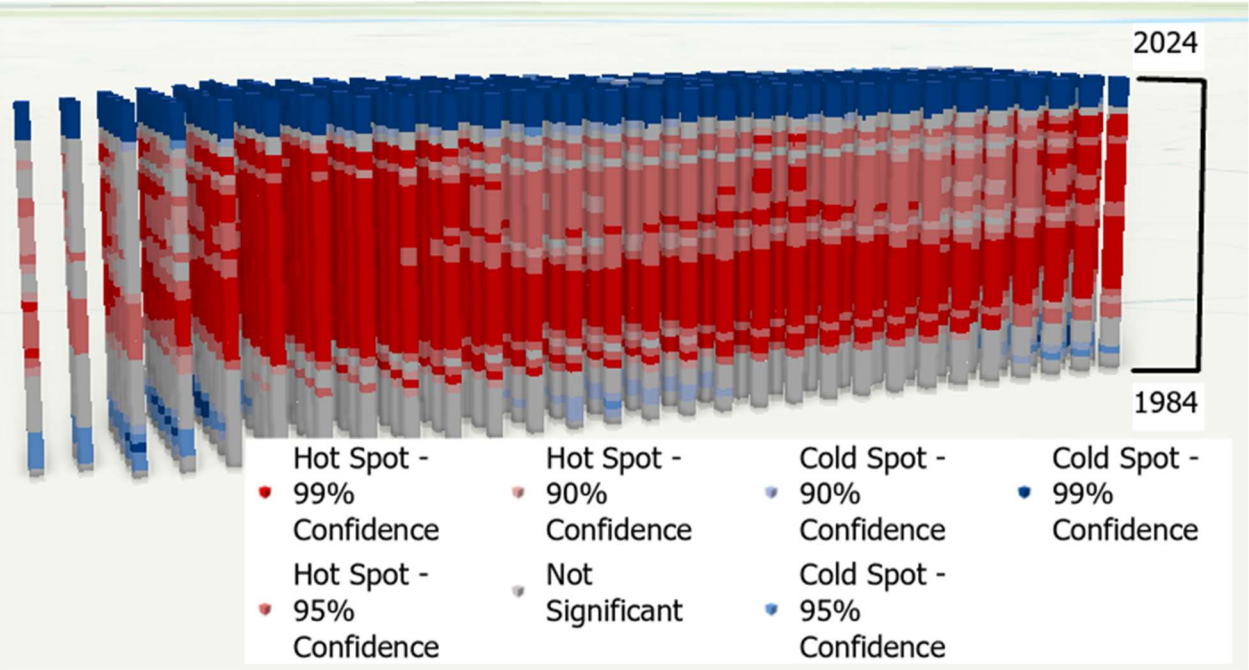

Figure 3.13. A cross section of oscillating cold spots present in the EHSA of WDNR.

GPNF Study Area

70% of GPNF NDVI pixels, a total of 63 km^2 , were determined to be oscillating hot spots and 4 km^2 were determined as a new hot spot (a pixed that is a hot spot in the final image and has never been a hot spot in previous images) (Esri b, n.d.). There was only 1 km^2 of GPNF found to be diminishing cold spots, and there was no new cold spot pattern on the GPNF (Figure 3.14a and 3.14b).

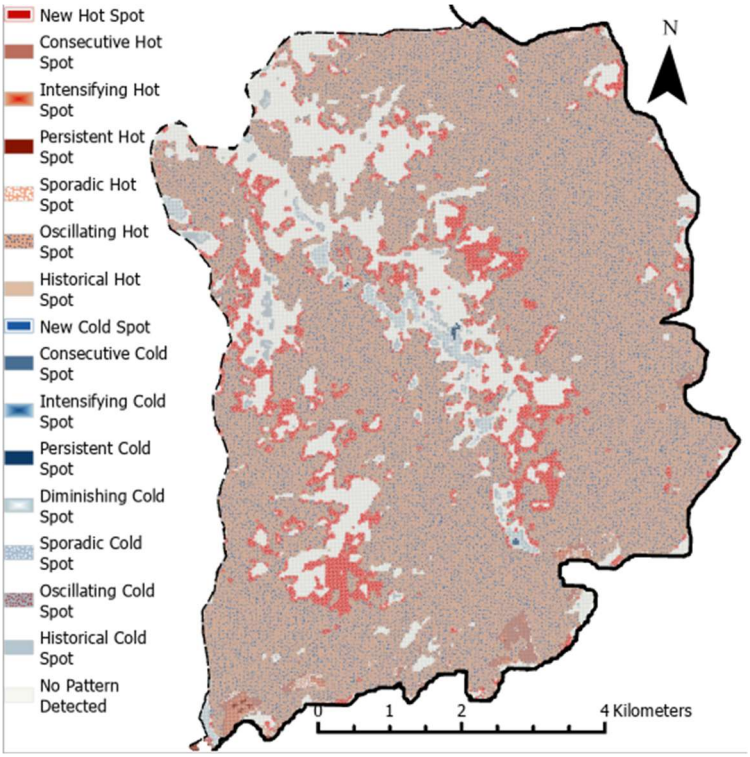

Figure 3.14a. GPNF South EHSA output.

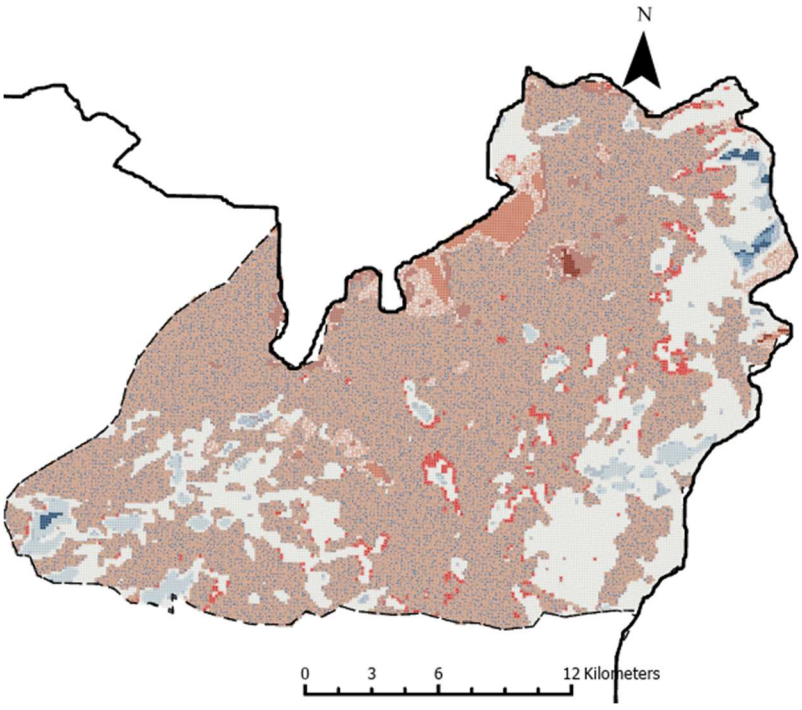

Figure 3.14b. GPNF North EHSA output.

WEYCO Study Area

Like the WDNR, the WEYCO management area contains 23 km^2 of oscillating cold spots. Interestingly, there are only 0.1 km^2 of intensifying hot spots (a pixel that has been a hot spot in at least 90% of the images, including the final image while the intensity of clustering of surrounding high NDVI values in each image is also increasing) (Esri b, n.d.). In other words, only 0.1 km^2 of the WEYCO management area has a trend of increasing NDVI each year and has neighboring NDVI pixels that are also continuing to increase. Contrary to the three previously analyzed management areas, WEYCO does have 0.5 km^2 of new cold spots. There are 73 km^2 of oscillating hot spots on WEYCO which mark the areas as statistically significant hot spots in the latest years (Figure 3.15).

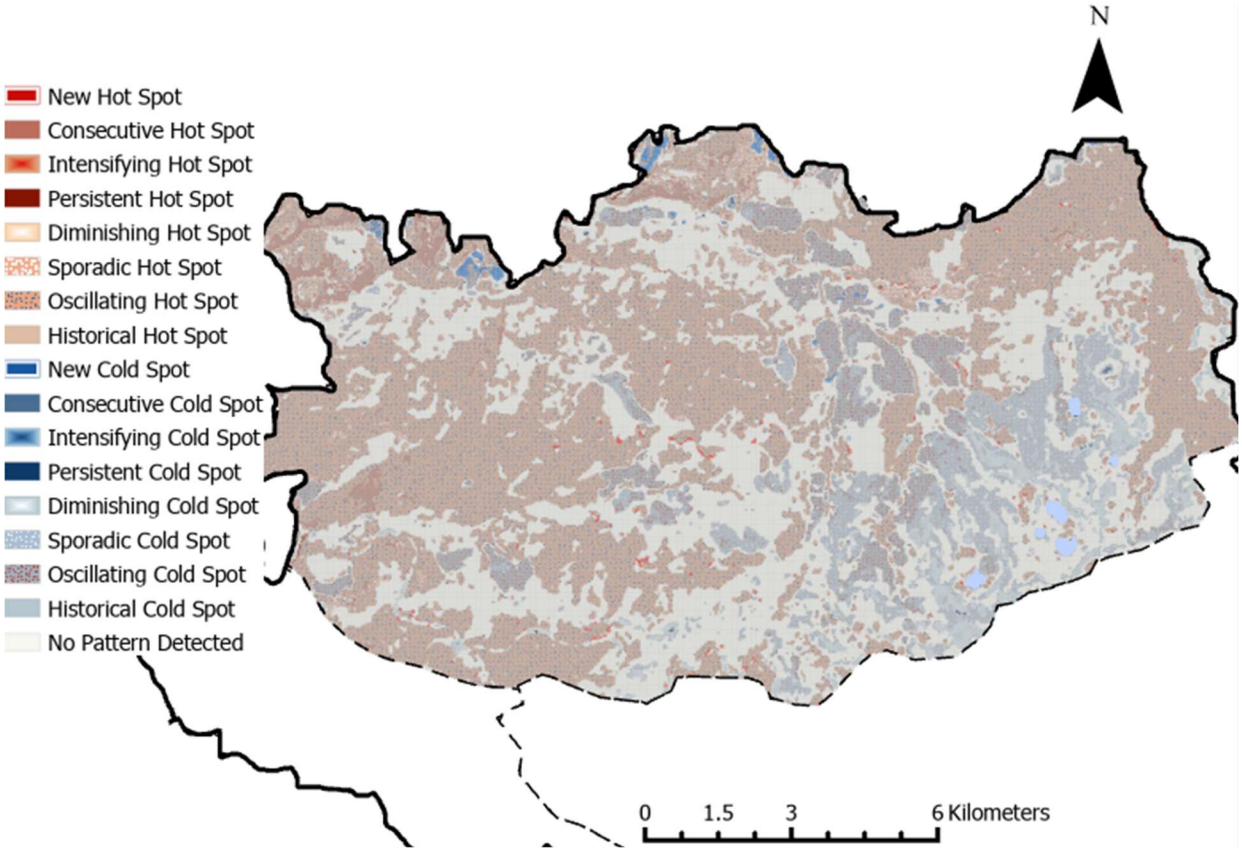

Figure 3.15. Weyco EHSA output.

3.5 Discussion

The objective of this study was to determine how vegetation has reestablished throughout the MSH BZ and on the various management areas. The management areas consist of WEYCO, WDNR, GPNF, and NVM. Using the EHSA allowed for an assessment of patterns of growth that have occurred across time and space for the various management areas from 1984 – 2024.

The initial analysis included 40 years of NDVI across the entire BZ. Most hot spots of growth are located on the WEYCO management area or the WDNR management area which is consistent with results from previous studies that assessed growth in the earlier years of reestablishment that were primarily the result of replanting (Marzen et al., 2011, and Harrington et al., 1998). However, the space-time cubes allow for additional analysis of how the changes occurred across time and space using space-time-cube bins. WEYCO holds 39% of persistent hot spots, 95% of historical hot spots, and 77% of the consecutive hot spots. Most new hot spots are present on the GPNF which is likely due to multi-purpose land use and delayed replanting efforts. These new hot spots have never had NDVI high enough to be a hot spot of growth until 2024. Over 93% of all diminishing cold spots are on the NVM (a pixel that has been a cold spot in 90 percent of the images, including the final image, but the intensity of clustering of surrounding low NDVI values is decreasing over time) (Esri b, n.d.).

The separate analysis of the NVM management area found that there were new hot spots near the crater and at higher elevations with steeper slopes. These areas are seeing a large enough increase in NDVI in the NVM study area to make them hot spots of vegetation in 2024. These new hot spots were also accompanied by diminishing cold spots

near the crater. These diminishing cold spots are areas that have low NDVI values, but the low NDVI values are beginning to increase with each time step. Therefore, they are potentially one time step away from becoming new hot spots if the NDVI values continue to increase. The exceptions of cold spots located away from the crater were primarily areas around the South and North Fork of the Toutle River and the Muddy River. The NVM is mostly covered with over 129 km^2 of oscillating hotspots which, when viewed as a cross section, show a pattern of increasing NDVI from 1984 to 2024.

There were only 10 km^2 of new hot spots on the WDNR management area, and they were near the NVM. All cold spot patterns were around the North Fork of the Toutle River. Conversely, the hot spot patterns can be found at higher elevations above the North Fork of the Toutle River. There has been some loss of vegetation and timber on WDNR, but this can be contributed to clear cutting timber operations. The oscillating cold spots gave these locations away as decreasing in NDVI over time as opposed to the increase in NDVI over time. Upon reviewing the NDVI imagery, the clear cutting on WDNR took place between the summer of 2019 and the summer of 2020 (Figure 3.16).

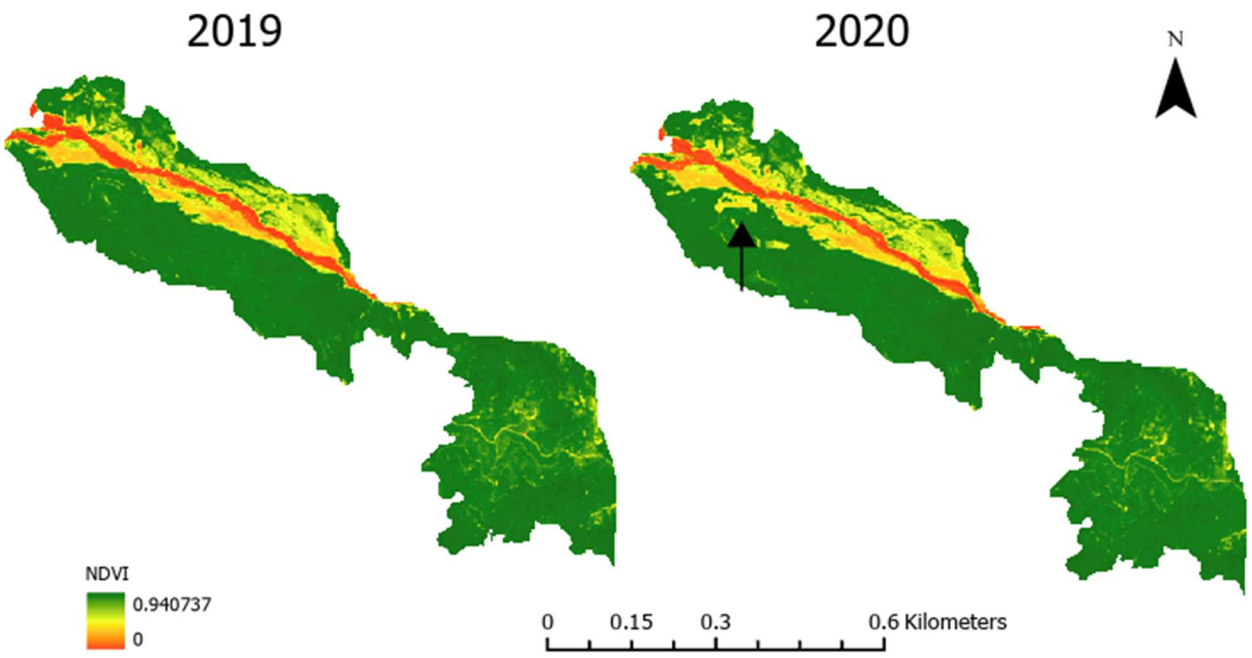

Figure 3.16. NDVI images showing minor timber operations that took place on WDNR between 2019 and 2020.

GPNF has the most consistent history of recovery. There are over 63 km^2 of oscillating hot spots on the 81 km^2 management area. These are areas with a consistent enough increase in NDVI over time to transform them from cold spots to hot spots of vegetation growth. This is a pattern that was expected as it highlights the reestablishment of vegetation over time. New hot spots can also be found in the GPNF where NDVI has seen a significant increase in 2024. There are only 2 km^2 of all cold spot patterns in the GPNF management area.

The WEYCO management area, on average, has the highest NDVI of any of the management areas, but the EHSA of WEYCO shows that portions of the property have had an inconsistent rate of reestablishment. Three patterns substantiate this observation, and they are the new cold spot, the oscillating cold spot, and the lack of intensifying hot

spots. New cold spots are present on the WEYCO management area where the NDVI has never been low enough to be a cold spot until 2024. Oscillating cold spots on WEYCO were hot spots in previous years but have since had several years of NDVI low enough that they have been determined to be cold spots. The lack of intensifying hot spots suggests that there are few hot spots of NDVI that are continuing to intensify every year. The additional three management areas WDNR, GPNF, and NVM contained more intensifying hot spots. Located beneath the oscillating cold spots were clear cut areas. The NDVI imagery showed that timber harvesting occurred on the property between the years 2010 and 2024 (Figure 3.17)

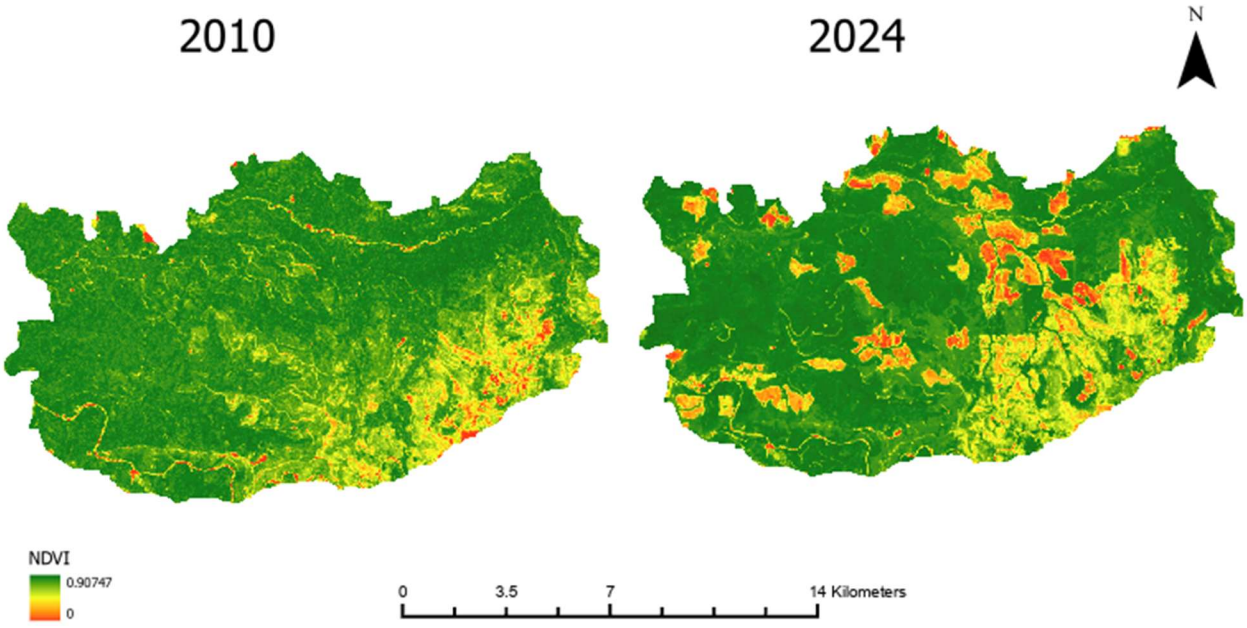

Figure 3.17. NDVI from 2010 and 2024 displaying timber operations that took place during the time period.

3.6 Conclusion

Through analysis of the entire BZ study area, the study found that the WEYCO management area holds the highest NDVI. In the river valleys and areas of the BZ closest to MSH on the NVM management area, the extent of vegetation is minimal, but growth is continuing to increase every year. Additionally, of the pixels that have had an NDVI increase significant enough to become new hot spots of vegetation growth, over 97% are located on the GPNF and NVM management areas. Upon analysis of the separate management areas, these patterns are further explained. While the WEYCO and WDNR management areas have a higher NDVI compared to the average of the entire BZ, they have experienced a more inconsistent rate of growth. This can be attributed to some minor timber harvesting activities that occurred between the years 2019 – 2020 on the WDNR management area and larger timber harvesting occurring between the years 2010 - 2024 on the WEYCO management area. The NVM and GPNF show a trend of consistently increasing growth. While they hold many cold spots of vegetation growth, many of these cold spots are diminishing. Thus, the conclusion of this study is that WEYCO and WDNR management areas have had the greatest extent of vegetation growth directly following the eruption, but the NVM and GPNF have the most consistent rate of growth. With no external interruptions to the growth of the NVM and GPNF vegetation, the properties will likely continue a similar trend of consistent growth as has occurred in the past 40 years. The growth of vegetation on the WDNR, and most certainly the WEYCO management area has been the most successful as they hold some of the highest NDVI values, but the growth on these properties will be dependent on the extent of timber operations as they appear to have resumed around 30 – 39 years after the eruption.

3.7 References

Abelairas-Etxebarria, P., & Astorkiza, I. (2020). From exploratory data analysis to exploratory spatial data analysis. *Mathematics and Statistics*, *8*(2), 82–86. https://doi.org/10.13189/ms.2020.080202

Blachowski, J., Dynowski, A., Buczyńska, A., Ellefmo, S. L., & Walerysiak, N. (2023). Integrated spatiotemporal analysis of vegetation condition in a complex post-mining area: Lignite mine case study. *Remote Sensing*, *15*(12), 3067. https://doi.org/10.3390/rs15123067

Cuba, N., Sauls, L. A., Bebbington, A. J., Bebbington, D. H., Chicchon, A., Marimón, P. D., Diaz, O., Hecht, S., Kandel, S., Osborne, T., Ray, R., Rivera, M., Rogan, J., & Zalles, V. (2022). Emerging hot spot analysis to indicate forest conservation priorities and efficacy on regional to Continental Scales: A study of forest change in Selva Maya 2000–2020. *Environmental Research Communications*, *4*(7), 071004. https://doi.org/10.1088/2515-7620/ac82de

Crawford, C. J., Roy, D. P., Arab, S., Barnes, C., Vermote, E., Hulley, G., Gerace, A., Choate, M., Engebretson, C., Micijevic, E., Schmidt, G., Anderson, C., Anderson, M., Bouchard, M., Cook, B., Dittmeier, R., Howard, D., Jenkerson, C., Kim, M., … Zahn, S. (2023). The 50-year Landsat Collection 2 Archive. *Science of Remote Sensing*, *8*, 100103. https://doi.org/10.1016/j.srs.2023.100103

Devananda, K., Reddy, C. S., & Arigela, R. K. (2024). Tracking five decades (1972–2024) of spatio-temporal dynamics and hotspots of Prosopis juliflora in Keoladeo National Park, a world heritage site. *Spatial Information Research*, *32*(6), 815–828. https://doi.org/10.1007/s41324-024-00598-6

Dwyer, J. L., Roy, D. P., Sauer, B., Jenkerson, C. B., Zhang, H. K., & Lymburner, L. (2018). Analysis Ready Data: Enabling Analysis of the Landsat Archive. *Remote Sensing*, *10*(9), 1363. https://doi.org/10.3390/rs10091363

Earth Resources Observation and Science (EROS) Center. (2020). Landsat 4-5 Thematic Mapper Level-2, Collection 2 [dataset]. U.S. Geological Survey. https://doi.org/10.5066/P9IAXOVV.

Earth Resources Observation and Science (EROS) Center. (2020). Landsat 8-9 Operational Land Imager / Thermal Infrared Sensor Level-2, Collection 2 [dataset]. U.S. Geological Survey. https://doi.org/10.5066/P9OGBGM6.

ESRI a. (n.d.). Emerging hot spot analysis (space time pattern mining). Emerging Hot Spot Analysis (Space Time Pattern Mining)-ArcGIS Pro | Documentation. https://pro.arcgis.com/en/pro-app/latest/tool-reference/space-time-pattern-mining/emerginghotspots.htm

ESRI b. (n.d.). How emerging hot spot analysis works. How Emerging Hot Spot Analysis works-ArcGIS Pro | Documentation. https://pro.arcgis.com/en/pro-app/latest/tool-reference/space-time-pattern-mining/learnmoreemerging.htm

Forest Health Monitoring. US Forest Service. (n.d.). https://www.fs.usda.gov/science-technology/forest-health-protection/monitoring

Harrington, L. M. B., Harrington, J. A., & Frenzen, P. M. (1998). Vegetation change in the mount st. helens (U.S.A.) Blast Zone, 1979–1992. *Geocarto International*, *13*(1), 75–82. https://doi.org/10.1080/10106049809354631

Harris, N. L., Goldman, E., Gabris, C., Nordling, J., Minnemeyer, S., Ansari, S., Lippmann, M., Bennett, L., Raad, M., Hansen, M., & Potapov, P. (2017). Using spatial statistics to identify emerging hot spots of forest loss. *Environmental Research Letters*, *12*(2), 024012. https://doi.org/10.1088/1748-9326/aa5a2f

Hossain, M. S., Bujang, J. S., Zakaria, M. H., & Hashim, M. (2015). Assessment of landsat 7 scan line corrector-off data gap-filling methods for seagrass distribution mapping. *International Journal of Remote Sensing*, *36*(4), 1188–1215. https://doi.org/10.1080/01431161.2015.1007257

Iverson, L. R., Graham, R. L., & Cook, E. A. (1989). Applications of satellite remote sensing to forested ecosystems. *Landscape Ecology*, *3*(2), 131–143. https://doi.org/10.1007/bf00131175

Krankina, O. N., DellaSala, D. A., Leonard, J., & Yatskov, M. (2014). High-biomass forests of the Pacific Northwest: Who manages them and how much is protected? *Environmental Management*, *54*(1), 112–121. https://doi.org/10.1007/s00267-014-0283-1

Lausch, A., Erasmi, S., King, D., Magdon, P., & Heurich, M. (2016). Understanding Forest Health with remote sensing -part I—a review of spectral traits, processes and remote-sensing characteristics. *Remote Sensing*, *8*(12), 1029. https://doi.org/10.3390/rs8121029

Lechner, A. M., Foody, G. M., & Boyd, D. S. (2020). Applications in remote sensing to Forest Ecology and Management. *One Earth*, *2*(5), 405–412. https://doi.org/10.1016/j.oneear.2020.05.001

Lee, R. J., & Chow, T. E. (2015). Post-wildfire assessment of vegetation regeneration in Bastrop, Texas, using landsat imagery. *GIScience & Remote Sensing*, *52*(5), 609–626. https://doi.org/10.1080/15481603.2015.1055451

Li, X., Yu, L., Xu, Y., Yang, J., & Gong, P. (2016). Ten years after Hurricane Katrina: Monitoring Recovery in New Orleans and the surrounding areas using remote sensing. *Science Bulletin*, *61*(18), 1460–1470. https://doi.org/10.1007/s11434-016-1167-y

Li, Z. (2022). Spatial distribution and temporal change of vegetation restoration after the eruption of Mount St. Helens: From 1984 to 2019. *Highlights in Science, Engineering and Technology*, *17*, 133–141. https://doi.org/10.54097/hset.v17i.2555

Mann, H. B. (1945). Nonparametric tests against trend. *Econometrica: Journal of the econometric society*, 245-259.

Marzen, L. J., Szantoi, Z., Harrington, L. M. B., & Harrington, J. A. (2011). Implications of management strategies and vegetation change in the mount st. helens blast zone. *Geocarto International*, *26*(5), 359–376. https://doi.org/10.1080/10106049.2011.584977

Navalgund, R. R., Jayaraman, V., & Roy, P. S. (2007). Remote sensing applications: An overview. *Current Science*, *93*(12), 1747–1766. http://www.jstor.org/stable/24102069

Nelson, M. D., McRoberts, R. E., Holden, G. R., & Bauer, M. E. (2009). Effects of satellite image spatial aggregation and resolution on estimates of forest land area. *International Journal of Remote Sensing*, *30*(8), 1913–1940. https://doi.org/10.1080/01431160802545631

Ord, J.K. and Getis, A. (1995), Local Spatial Autocorrelation Statistics: Distributional Issues and an Application. Geographical Analysis, 27: 286-306. https://doi.org/10.1111/j.1538-4632.1995.tb00912.x

Pflugmacher, D., Cohen, W. B., & E. Kennedy, R. (2012). Using landsat-derived disturbance history (1972–2010) to predict current forest structure. *Remote Sensing of Environment*, *122*, 146–165. https://doi.org/10.1016/j.rse.2011.09.025

Prabakaran, C., Singh, C. P., Panigrahy, S., & Parihar, J. S. (2013). Retrieval of forest phenological parameters from remote sensing-based NDVI time-series data. *Current Science*, *105*(6), 795–802. http://www.jstor.org/stable/24097517

Rochelle, J. A., Ford, R. L., & Terry, T. A. (1992). The Reforestation Challenge. *Journal of Forestry*, *90*(5), 20–24. https://doi.org/10.1093/jof/90.5.20

Snellgrove, T. A., Kendall Snell, J. A., & Max, T. A. (1983). Damage to national forest timber on Mount St. Helens. *Journal of Forestry*, *81*(6), 368–371. https://doi.org/10.1093/jof/81.6.368

Shaw, G., & Burke, H. K. (2003). *Spectral imaging for Remote Sensing*. Lincoln Laboratory Journal. 14. https://www.researchgate.net/publication/250260467_Spectral_Imaging_for_Remote_Sensing

Teltscher, K., & Fassnacht, F. E. (2018). Using multispectral landsat and sentinel-2 satellite data to investigate vegetation change at Mount St. Helens since the Great Volcanic eruption in 1980. *Journal of Mountain Science*, *15*(9), 1851–1867. https://doi.org/10.1007/s11629-018-4869-6

US Army Corps of Engineers. (2020). *Mount St. Helens Erupts and USACE Responds*. U.S. Army Corps of Engineers Headquarters. https://www.usace.army.mil/About/History/Historical-Vignettes/Relief-and-Recovery/137-Mt-St-Helens/

USFS's Gifford Pinchot National Forest - Monitor Ridge Climbing Route. Forest Service National Website. (n.d.) https://www.fs.usda.gov/recarea/giffordpinchot/recreation/recarea/?recid=31604

USFS's Planning rule - home. Forest Service National Website. (n.d.). https://www.fs.usda.gov/detail/planningrule/home/?cid=stelprdb5359471

WDNR's 2022-25 strategic plan: WA - DNR. WA. (n.d.). https://www.dnr.wa.gov/strategicplan

Xie, Y., Sha, Z., & Yu, M. (2008). Remote sensing imagery in vegetation mapping: A Review. *Journal of Plant Ecology*, *1*(1), 9–23. https://doi.org/10.1093/jpe/rtm005

Xu, B., Qi, B., Ji, K., Liu, Z., Deng, L., & Jiang, L. (2022). Emerging hot spot analysis and the spatial–temporal trends of Ndvi in the Jing River Basin of China. *Environmental Earth Sciences*, *81*(2). https://doi.org/10.1007/s12665-022-10175-5

Zhou, M., Li, D., Liao, K., & Lu, D. (2023). Integration of landsat time-series vegetation indices improves consistency of change detection. *International Journal of Digital Earth*, *16*(1), 1276–1299. https://doi.org/10.10

Chapter 4: The Influence of Environmental Variables on Forest Stand Attributes at MSH

4.0 Introduction

The Food and Agriculture Organization of the United Nations (FAO, 2025) commonly uses canopy height as a forest structure attribute to define forests worldwide. This definition highlights the importance of forest canopy height as this forest stand attribute holds a primary role in defining worldwide forests. Forest canopy height and NDVI are some of the most useful variables in estimating above ground biomass which is a predictor of overall forest stand productivity as well as carbon sequestration (Nurhidayat et al., 2023; `Ma et al., 2024). Ultimately, exploring the relationship between that of forest stand attributes such as canopy height, NDVI, and other environmental variables can lead to a better understanding of what factors drove the development of these attributes (Gadow et al., 2011). Studies often use regression analysis to determine the nature of these relationships, and commonly find variables such as topography, climate and soil disturbances affecting growth (Rahman et al., 2021).

The most relevant example to this study in the Mount St. Helens (MSH) Blast Zone (BZ) is that of Lawrence and Ripple (2000). This study utilized regression tree analysis to compare relationships of optical imagery indices of vegetation and assessed this growth in comparison to various environmental variables in the National Volcanic Monument (NVM) where vegetation was allowed to naturally reemerge. Following the 1980 eruption when forested areas were devastated at MSH, the study found that variables including slope, elevation, ash depth, and distance from the crater affected early re-establishment for plants and trees.

Many studies have explored the effects of the presence of volcanic ash on vegetation and tree reestablishment. In a specific study at MSH, Radwan & Campbell (1981) found seeds of all tree species began to grow well in soil, ash, and mud, but as time progressed, ash imposed significant challenges on seedling growth. At MSH, it was determined the areas that had the greatest chance at successful replanting were in those areas with shallower ash deposits (Marzen et al. 2011). In areas where natural growth was allowed to occur such as in the NVM ash impeded vegetation reestablishment.

Several studies discuss how topographic variables and in particular slope and elevation had an impact on ash depth and vegetation reestablishment (Frenzen 1992, Harrington et al, 1998, Marzen et al 2011). In planted areas, the ash deposits accumulated at lower elevations with gentler slopes which made it difficult to replant, whereas in areas of natural regrowth, steeper slopes were likely to have ash erode allowing vegetation to survive the eruption and thus in those steeper slope locations it was more likely to have vegetation reestablishment.

Another topographical factor that can influence vegetation growth is aspect or the direction slopes face. Hillshade GIS layers represent daily and seasonal solar radiation exposure as a function of slope azimuth direction and elevation. A hillshade layer is a direct representation of how much sun an area is exposed to, but the effect that sunlight abundance has on the environment varies in different study areas. Leaf exposure to sun is generally best for trees, but in some cases increased sun exposure can deplete water availability (Xian et al., 2024). Nevertheless, studies confirm that sun exposure, as modeled by hillshade, often plays a critical role in controlling forests and vegetation growth (Najafifar et al., 2019).

The previous studies mentioned above primarily used satellite imagery to analyze vegetation regrowth at MSH using multispectral data from several bands of the

electromagnetic spectrum and this has been the main source of data collected using RS since 1980 at MSH. One of the more recent technologies for collecting RS data is through Light Detection and Ranging (LiDAR). This will be the first study to use LiDAR in a landscape scale analysis at MSH. An analysis of the BZ vegetation using LiDAR will add to previous studies by providing an estimate of tree growth and potentially associated characteristics of tree health that can be derived from tree height.

Ground based methods of measuring tree canopy attributes such as canopy height often involve some level of difficulty and produce results of unknown error given that vegetation, or other tree canopies interfere with making accurate measurements from the ground up (Sibona et al., 2016). Ground sampling canopy height information is time consuming, and spatially extensive ground sampled canopy height data is rare. With advancements in RS technology, there are other options for estimating canopy height. Wang et al. (2019) and Sibona et al. (2016) found that traditional methods of field measurements of canopy height often overestimate, especially in dense forests, and Airborne Laser Scanning (ALS) improved the canopy height measurement accuracy over the traditional methods. ALS was first developed in the 1970s and 1980s in the United States and Canada for creating accurate Digital Terrain Models (DTMs) (Ackermann, 1999). ALS is a form of active RS that uses lasers to measure heights and distances. The first return from when the laser contacts an object will be the highest object above the ground. Any of the following returns capture additional information about shorter objects until the last return measures the distance to the ground (Camarretta et al., 2019). Several countries have since completely adopted ALS as acceptable for extracting canopy models of forest stand attributes including Finland, Norway, Sweden, Canada, and the United States (Fassnacht et al., 2023).

Leveraging ALS data and GIS, derivative models can be created to gather information from an area of interest. A DTM is one of the most common uses of ALS data. A DTM is simply a raster data model representing ground elevation. To create a DTM, the last points or returns from ALS data are used. A Digital Surface Model (DSM) considers the points that are above the ground (vegetation, structures, power lines etc.), and it is created using the first laser returns from ALS. A subtraction of DTM raster values from the DSM raster values on a cell-by-cell basis creates a Canopy Height Model (CHM) (Oh et al., 2022). Top canopy structure such as that modeled by a CHM generally maintain high accuracies across literature, but the accuracy of ALS derived forest structure models does decrease when they are implemented to try and assess forest structure attributes present below the canopy (Kelly et al., 2017).

ALS data was collected for the entire MSH BZ primarily from 2017 to 2018 during leaf-on periods. Though these ALS data exist, this is the first study to use canopy height to develop environmental models of vegetation growth in the BZ. Previous RS studies were limited to forest stand attributes only derived from optical imagery, and thus there is a gap in knowledge on the BZ canopy height. This study uses a CHM and 10m NDVI imagery to assess the strength of relationships of CHM and NDVI with environmental drivers (slope, ash depth, hillshade, elevation, and distance from crater) using multiple linear regression.

4.1 Study Area

The study area consists of the Weyerhaeuser Company (WEYCO), Gifford Pinchot National Forest (GPNF), National Volcanic Monument (NVM), and Washington Department of Natural Resources (WDNR) management areas. These management boundaries identified in Harrington et al. (1998) and Marzen et al. (2011). These studies

argue that analysis of the entire BZ must be conducted with the knowledge that management areas have been managed for different purposes and thus the extent of the growth can vary accordingly. These boundaries have been used to delineate study areas by Marzen et al. (2011) and have been verified through Washington State Geoservices (2024) (Figure 4.0).

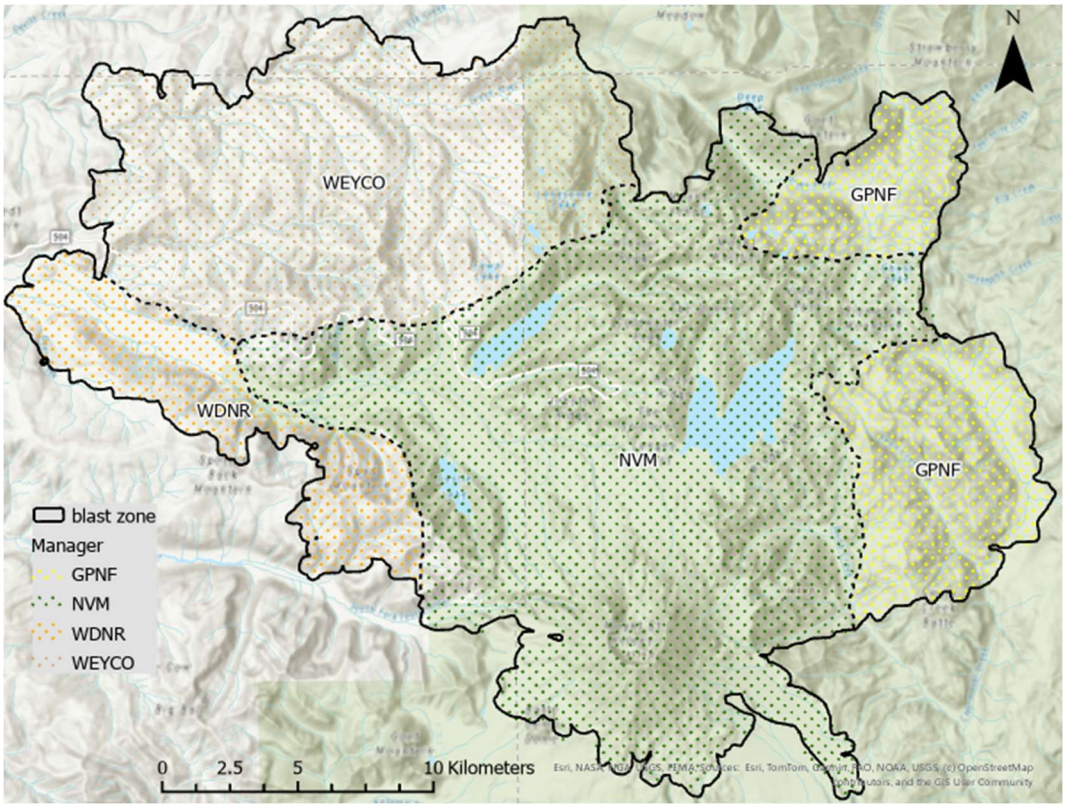

Figure 4.0: This is a map of the blast zone, and the different property managers that lie within it. Boundary information courtesy of Washington State Geoservices (2024) and Marzen et al. (2011)

4.2 Research Objectives

Objective 2

The first objective of this chapter and second of the study is to use available LiDAR derived data to develop a CHM for the study area which allows for comparison of canopy height on all four of the defined management areas.

Completing Objective 2 will answer the following research question:

Q2. What is the relative canopy height in each management area as determined by ALS derived data?

Objective 3

The third objective of this study is to utilize LiDAR-derived canopy height information as well as 10m NDVI values gathered in the same year to explore variables that have influenced the reestablishment of the vegetated and forested areas. Independent variables such as elevation, slope, ash depth, and hillshade will be tested against canopy height and the NDVI values in regression analysis.

Completing Objective 1 will answer the following research question:

Q3. What environmental variables were the drivers of reestablishment?

Hypothesis 1 – Hypothesis 5 are built around research question 3. These hypotheses present variables that are believed to influence reestablishment and list the reasoning for the assumed relationship. The hypotheses are listed below.

Hypothesis 1:

Slope will have a positive effect on NDVI and CH. This hypothesis is grounded in the knowledge that ash on steeper slopes weathers away faster thus soil availability is more

prominent and reachable by the root structure of vegetation on steeper slopes. In planted areas, this would mean that newly planted vegetation would have a greater chance at finding root in soil. In the NVM, steeper slopes were more likely to have surviving vegetation due to the weathering of ash. Root structure was able to spread from these areas of surviving vegetation.

Hypothesis 2:

Ash depth will have a negative effect on NDVI values and Canopy Height (CH). This presumption is based off the knowledge that root structure was limited to soil availability in areas where ash depth was greater, and this effect prevented the root structure from absorbing organic material or otherwise responding to an established soil horizon besides that of the deposited volcanic ash. Ash depth in the NVM affected the spread of surviving vegetation. Areas with less ash were more likely to spread from preexisting vegetation. In areas that were replanted, managers focused on replanting where ash depth was minimal because workers were able to plant seedlings in in the nutrient-rich soil by digging through lower amounts of ash.

Hypothesis 3:

Hillshade will have a positive effect on both NDVI and CH. This relationship is presumed given the knowledge that vegetation, when given the availability of more sunlight, will have a more significant rate of growth given that sunlight is a key component of photosynthesis.

Hypothesis 4:

This study theorizes that elevation will have a negative relationship with NDVI values and CH. Lawrence and Ripple (2000) theorized that elevation would not affect revegetation. However, their findings concluded that lower elevations correlated with greater revegetation in the later years of their analysis which ran from 1984-1995.

Hypothesis 5:

Distance from the crater will have a positive relationship with NDVI and CH values. This relationship is expected because of the extent of the damage imposed upon the area by the eruption. Growth closest to the crater is most likely to see lingering negative effects.

4.3 Methods

4.3.1 Data

CHM, DTM, and DSM Data Processing

The ALS point cloud derived models including Digital Terrain Model (DTM), Digital Surface Model (DSM) were downloaded from the Washington State LiDAR Portal (WDNR n.d.). The ALS datasets used to create these models consist of flights from the Washington FEMA 3DEP 2018 LiDAR (USGS, 2019), Washington FEMA 3DEP 2017 LiDAR (USGS, 2017), and the Southwest Washington LiDAR (WDNR, 2017). The accuracy of the Lidar data was a process that was conducted by federally approved data vendors using many different software and ground-based techniques in order to meet Federal Geographic Data Committee (FGDC) standards. The USGS and WDNR do not always collect their own spatial data, especially ALS, rather they contract these jobs out to certified geospatial data providers and collectors. The USGS (2019) and USGS (2017) ALS were collected and processed by Quantum Spatial Inc., and the WDNR (2017) was collected and processed by Geoterra Inc. All the ALS data meets FGDC standards.

Compared to satellite collected data, ALS data are not as readily available, and it can be very expensive to collect. The advantages of ALS data are the improved spatial resolution when compared to publicly available satellite optical imagery as well as the ability of ALS to obtain height information (Pflugmacher et al., 2012). Given that ALS data collection and use

is still relatively new technology, there are concerns about data accuracy and integrity, so it is important to gather ALS data from reputable data vendors who include accuracy assessments (Fassnacht et al., 2023). The United States has made significant strides in developing its National Spatial Data Infrastructure (NSDI), which is managed by the Federal FGDC. The goal of the FGDC is to coordinate the creation and collection of accurate spatial data among federal and local governments (Kok & van Loenen, 2005).

One requirement of the FGDC is that data collectors provide accuracy assessments with their datasets so that the effectiveness of the data to produce acceptable analysis is clear. Part of the purpose of the ground control surveys is to establish land cover class checkpoints which aid in the classifications of ALS returns which were completed by the data collection companies. Geoterra and Quantum Spatial actively assess their data accuracy which includes ground control surveys and the placement of ground control points. Upon collecting the data, multiple software was used by Quantum Spatial and Geoterra to process the LiDAR to extract the DTM and DSM derivative models which had a spatial resolution of 1 meter. This software consisted of Terra Scan, Terra Match, Terra Modeler, Waypoint inertial explorer, Leica Cloud Pro Explorer, and others. The processing included GPS control computations, smoothed best estimate trajectory calculations, kinematic corrections, calculation of laser point position, sensor calibration, and LiDAR point classifications. Following processing, point cloud density and accuracy assessments were completed (USGS, 2019, USGS, 2017, WDNR, 2017). USGS (2017) reported a vertical Root Mean Squared Error (RMSE) of 0.069 meters, USGS (2019) reported a vertical RMSE of 0.045 meters, and WDNR (2017) reported a vertical RMSE of 0.060 meters.

Sentinel - 2 Level 2A NDVI

A Sentinel - 2 Level 2A NDVI image (Programme of the European Union, 2017) was created as one of the dependent variables. The image, collected by the sensor on August 26, 2017, was filtered to 10% cloud cover. The Sentinel – 2 Level 2A are surface reflectance products which have been available since 2016. Like the Landsat Level 2 Collection 2, Sentinel – 2 Level 2A are Analysis Ready Data. The MAJA Level-2A processor is used to process the images once they are collected. The process includes error corrections for molecular absorption, clouds, cloud shadows, and other atmospheric influence (Hagolle et al., 2021). The choice to use Sentinel imagery for this chapter instead of Landsat imagery was made solely on the basis that these images have a $10m^2$ spatial resolution as opposed to the Landsat $30m^2$ resolution.

Hillshade

The hillshade models were created by Quantum Spatial and Geoterra as part of the completion for gathering the USGS (2019), USGS (2017), and WDNR (2017) data. Hillshade models are created by using elevation and azimuth information. The resulting layer has image bit values ranging from 0 – 255 where 0 represent no light availability and 255 represents the maximum available light availability. These hillshade models had 1-meter spatial resolution. It is posited that vegetation growth is greater in areas with higher hillshade values.

Elevation

The processed DTMs from USGS (2019), USGS (2017), and WDNR (2017) were mosaicked to provide an elevation model for the study area. These models were created from the ALS processing completed by Quantum Spatial and Geoterra. This model represents elevation in feet, and the spatial resolution was 1 meter. It is hypothesized that vegetation

growth is greater at lower elevations.

Slope

A 1-meter spatial resolution slope model was derived from the study area DTM. This model uses the changes in elevation values to determine the percent rise from pixel to pixel. A 0 degree slope represents a completely flat piece of ground while a 90 degree slope represents a maximum incline. It is posited that vegetation growth is greater on steeper slopes.

Ash Depth

An isoline ash depth map in centimeters (ranging from x to x) created by a U.S. Department of the Interior USGS geological survey (Waitt et al., 1981) in the summer of 1980 following the eruption was geometrically corrected and rasterized to a spatial resolution of 20 meters using GIS. It is posited that vegetation growth is greater with lower ash depth.

Distance From The Crater

The exact location of the crater of the 1980 eruption was derived from Lipman & Mullineaux (1981). A 20m Distance raster was created where every cell value indicated the distance from the crater. It was theorized that with increased distance from the crater, vegetation growth is greater.

4.3.2 Analysis

This study employed Multiple Linear Regression (MLR) to assess the relationships between multiple independent variables and the dependent variables NDVI and CHM on the management areas. This method was chosen because we expect to see linear relationships between hillshade, ash depth, elevation, distance from the crater, slope, and the dependent variables (NDVI, CHM). Linear regression analysis quantifies the linear

relationship between a dependent variable and independent variables. The adjusted R^2 value accounts for the addition of multiple independent variables and is generally lower in absolute value than the standard R^2 value (Ozili, 2022). Independent variable coefficients were used to determine the effects of the various variables in the MLR. These coefficients are vital to the interpretation of the model because they represent the relationships between variables and whether they are positively or negatively related (Bazdaric et al., 2021). The significance of these relationships was validated using p-values < 0.05, and the t statistic test determined by the spatial analysis software ArcGIS Pro Version 3.4. Multicollinearity occurs when independent variables are correlated to each other and are playing redundant roles in the model. To measure multicollinearity, this study employed the Variance Inflation Factor (VIF). VIF values above 10 suggest that there is multicollinearity occurring between variables. VIF values are most needed in studies where there are many independent variables (Senaviratna & A. Cooray, 2019). To complete the sampling of the CHM, NDVI, and independent variables for analysis, random points were generated proportional to land management areas using a random point generator in ArcGIS Pro version 3.4 In total 12,000 random sample points were extracted from the NVM, 10,000 were extracted from the WEYCO management area, and 4,000 random sample points were extracted from the GPNF and WDNR management areas.

4.4 Results

Summary of CH

One objective of this study was to present a CHM to assess differences in CH between the different management areas. The CHM was created using ALS derived DSM and DTM models which were collected by Quantum Spatial Inc. and Geoterra Inc. The maximum

CHM values were 287.9 ft for NVM, 282.9 ft for WEYCO, 268.8 foot for GPNF, and 237.4 ft for WDNR. However, these max heights fell well above the mean heights for the properties. The mean heights were 13.0 ft on NVM, 52.3 ft on WEYCO, 42.0 ft on WDNR, and 32.36 ft on GPNF. Only 0.113 km^2 of the CHM is over 100 ft tall, and only 0.0007 km^2 is over 200 ft tall. 0.0006 km^2 of the CHM which is greater than 200 ft, is located on the far east side of the NVM only 5.81 km away from the crater (Figure 4.1)

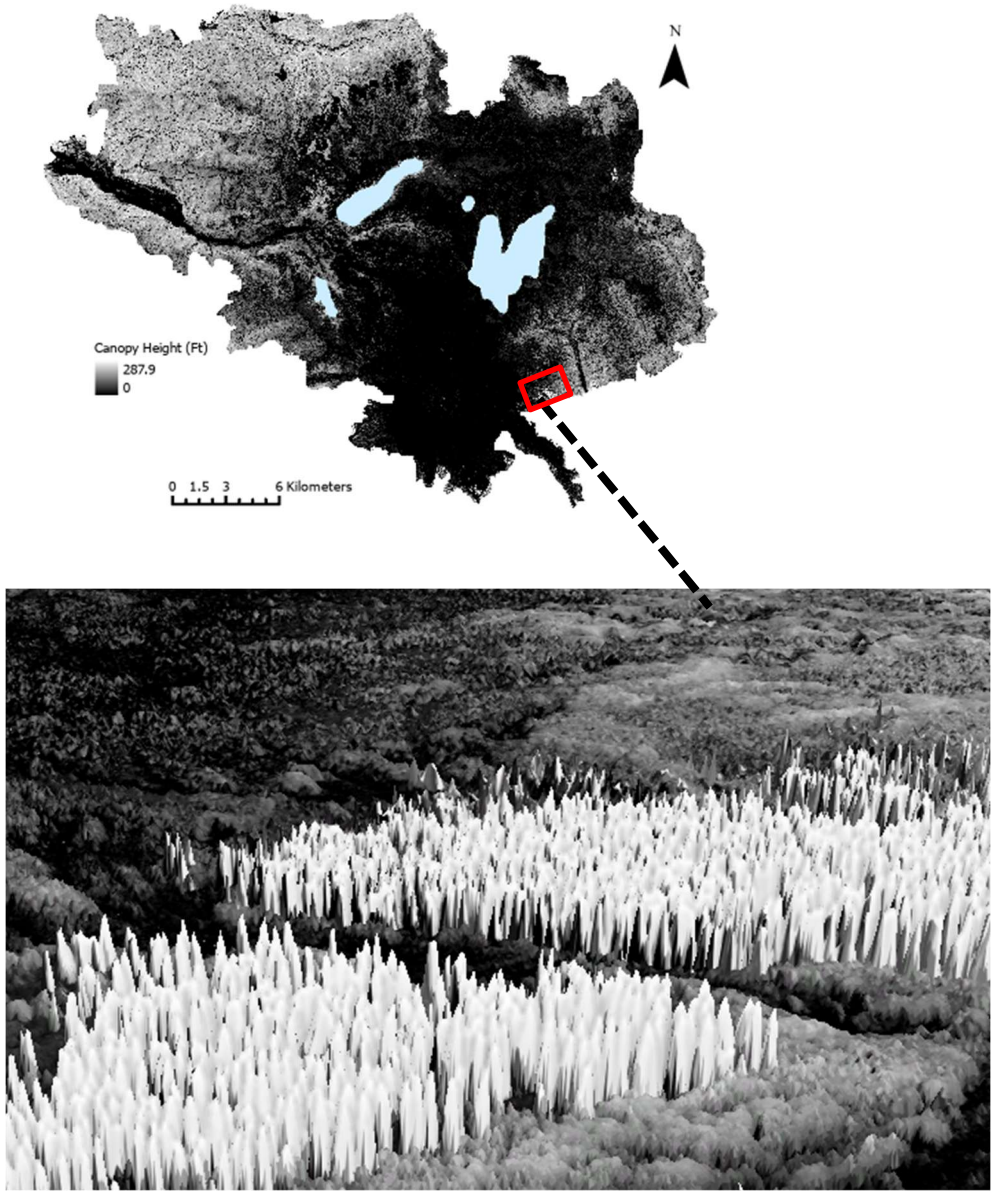

Figure 4.1. Old growth forest at NVM.

Model Interpretation NVM

The CH regression model for NVM produced an adjusted R^2 value of 0.31 meaning that the model explained 31% of the CH variation. All the variables had VIF values less than 2 (no multicollinearity), and p – values were less than 0.05. . As posited, Both ash depth and elevation had a negative relationship with CH. Slope had the greatest positive effect on CH with a coefficient of 0.19 while elevation had the greatest negative effect with a coefficient of -0.47 (Table 4.0).

Table 4.0. The table of results for the NVM-CH regression model. * indicates significant variable.

Variable	Coefficient	Std. Error	T Statistic	P - Value
Slope	0.192754	0.009724	19.821595	0.000000*
Hillshade	0.117142	0.009456	12.388393	0.000000*
DistFromCrater	0.080739	0.008916	9.055319	0.000000*
Elevation	-0.471370	0.008723	-54.038506	0.000000*
Ash Depth	-0.194787	0.008570	-22.728781	0.000000*

The NDVI model for the NVM had an adjusted R^2 value of 0.49 and therefore it best predicted the outcome that slope, hill shade, distance from crater, elevation, and ash depth had on NDVI. The p-values for the model and variables were all less than 0.05 indicating significant relationships. Elevation and ash depth both had a negative relationship with NDVI, and the variable with the most significant effect on NDVI was distance from the crater which had a positive coefficient of 0.45 (Table 4.1).

Table 4.1. The table of results for the NVM-NDVI regression model. * indicates significant variable.

Variable	Coefficient	Std. Error	T Statistic	P - Value
Slope	0.218992	0.008287	26.427272	0.000000*
Hillshade	0.183358	0.008058	22.755846	0.000000*
DistFromCrater	0.449589	0.007598	59.173544	0.000000*
Elevation	-0.359336	0.007433	- 48.343717	0.000000*
Ash Depth	-0.130893	0.007303	-17.923499	0.000000*

Model Interpretation WEYCO

The adjusted R^2 value for the WEYCO management area CH regression model was 0.40. All variables had significant p – values, and elevation and depth had negative relationships with CH. The largest VIF value was 4.21 for the distance from crater variable. Slope and hill shade had the strongest positive relationship indicating that steeper slopes with more sun exposure are more likely areas to produce taller CH (Table 4.2).

Table 4.2. The table of results for the WEYCO-CH regression model. * indicates significant variable.

Variable	Coefficient	Std. Error	T Statistic	P - Value
Slope	0.137427	0.008914	15.416883	0.000000*
Hill shade	0.116223	0.008768	13.255888	0.000000*
DistFromCrater	0.091686	0.016897	5.426022	0.000000*
Elevation	-0.317023	0.015618	-20.298970	0.000000*
Ash Depth	-0.274563	0.013586	-20.208555	0.000000*

The successful model for WEYCO NDVI had a p-value of less than 0.05 and all independent variables had a p-value of less than 0.05. Hillshade and distance from crater had an insignificant effect on NDVI with p-values greater than 0.05, so therefore these variables were excluded from the model. The remaining variables had significant relationships with NDVI and produced a regression model with an adjusted R^2 value of 0.20. The VIF values for the variables were all less than three, and the strongest relationships to NDVI were with ash depth and slope (Table 4.3)

Table 4.3. The table of results for the WEYCO-NDVI regression model. * indicates significant variable.

Variable	Coefficient	Std. Error	T Statistic	P - Value
Slope	0.059211	0.010321	4.923484	0.000002*
Elevation	-0.050815	0.018083	-3.274484	0.001079*
Ash Depth	-0.390505	0.015731	-24.824137	0.000000*

Model Interpretation GPNF

The finalized GPNF CH regression model proved to be significant with a p – value of less than 0.05. However, not all the variables held significant relationships with p – values less than 0.05. The slope and distance from crater variables had p-values greater than 0.05, and therefore, they were removed from the model. The final variables affecting CH were hill shade, elevation, and ash depth. The adjusted R^2 value for the model was 0.34. Elevation showed to have a strong negative relationship with CH here, and ash depth also had a negative relationship (Table 4.4).

Table 4.4. The table of results for the GPNF-CH regression model. * indicates significant variable.

Variable	Coefficient	Std. Error	T Statistic	P - Value
Hill shade	0.067992	0.014178	4.795701	0.000003*
Elevation	-0.557910	0.014198	-39.293873	0.000000*
Ash Depth	-0.112623	0.014218	-7.921355	0.000000*

The GPNF NDVI regression model proved significant with a p – value of less than 0.05, and additionally, every variable had a p – value indicating a significant relationship as well as VIF values less than 2. The adjusted R^2 value for the final model was 0.25. Elevation and ash depth both had negative relationships with NDVI, and both slope and hillshade had positive relationships with NDVI values (Table 4.5).

Table 4.5. The table of results for the GPNF-NDVI regression model. * indicates significant variable.

Variable	Coefficient	Std. Error	T Statistic	P - Value
Slope	0.131194	0.017259	7.601673	0.000000*
Hill shade	0.273250	0.016547	16.513642	0.000000*
DistFromCrater	0.101113	0.018929	5.341565	0.000000*
Elevation	-0.424354	0.016499	-25.719438	0.000000*
Ash Depth	-0.110300	0.018232	-6.049813	0.000000*

Model Interpretation WDNR

After removing elevation as a variable, the regression model comparing CH to the dependent variables produced a significant t statistic with a p - value < 0.05 and thus the model is valid to be assessed. The adjusted R^2 value was 0.22. All the independent variables had significant t - statistics with p - values < 0.05. There was no multicollinearity occurring between the variables with the largest of the VIF values being only 4.66 for the distance from crater variable. All independent variables had positive relationships with the dependent variable except for ash depth which had, as expected, a negative relationship with CH (Table 4.6).

Table 4.6. The table of results for the WDNR-CH regression model. * indicates significant variable.

Variable	Coefficient	Std. Error	T Statistic	P - Value
Slope	0.461246	0.014556	31.688260	0.000000*
Hillshade	0.183939	0.014635	12.568383	0.000000*
DistFromCrater	0.120317	0.021901	5.493656	0.000000*
Ash Depth	-0.269366	0.015408	- 17.482372	0.000000*

The regression model comparing NDVI to the dependent variables produced a significant t - statistic with a p - value of 0.000305 and the adjusted R^2 value was 0.31. The highest VIF value of all variables was 4.60 for the distance from the crater variable, and the only variable which had a negative relationship with NDVI was Ash Depth (Table 4.7).

Table 4.7. The table of results for the WDNR-NDVI regression model. * indicates significant variable.

Variable	Coefficient	Std. Error	T Statistic	P - Value
Slope	0.329168	0.013714	24.001663	0.000000*
Hillshade	0.091079	0.013789	6.605161	0.000000*
DistFromCrater	0.085028	0.020635	4.120528	0.000045*
Elevation	0.435793	0.018394	23.693789	0.000000*
Ash Depth	-0.102216	0.014517	-7.041022	0.000000*

4.5 Discussion

Linear Regression

Within the entire BZ, growth on all properties was affected by slope. The only model that did not see a significant relationship between CH and slope was the GPNF CH regression model. Therefore, the assumption that these variables had any effect on CH at GPNF must be removed. Slope did however have a significant effect on NDVI at GPNF. The relationship between slope and growth on the properties was always positive indicating that steeper slopes held higher NDVI or CH values. The most significant influence that slope had on growth was found at the WDNR management area where the coefficient value for the CH model was 0.46. The least significant influence that slope had on the dependent variables was found at the WEYCO management area where the slope coefficient value for the NDVI model was 0.06. Ash was absent on steeper slopes sooner after the eruption. The ash did not settle on steeper slopes as well as gentler slopes and was weathered away faster, so the positive relationship between growth and slope is believed to be in relation to the vegetation response to ash. This substantiates *Hypothesis 1* of the study.

Ash depth negatively effected the dependent variables on all management areas with significance of p-values <0.05 in every model. While not having the most negative influence on the dependent variables in every model (coefficients ranging from -0.11 to -0.39), ash depth was the only variable that consistently negatively affected growth across all management areas. Therefore, the relationship between ash depth and growth can be seen as negative throughout the BZ. Areas with greater ash deposits following the 1980 eruption have maintained lower CH and NDVI than areas with lesser ash deposits. These findings are consistent with *Hypothesis 2* of the study which posited that ash depth would have a negative relationship with vegetation growth. The negative relationship between vegetation growth and ash depth was likely due to different reasons in planted areas verses the NVM. Planting occurred more often in areas with little ash given that survival was considered more likely there. Vegetation present in NVM was more likely to survive and lead reestablishment in areas with less ash where root structure could spread.

Hillshade had positive relationships with NDVI and CH in every model except that of the WEYCO NDVI. These findings are consistent with *Hypothesis 3* which stated that areas with availability to more sun would see higher NDVI and CH values. However, we must reject the hypothesis that hillshade affected NDVI values on WEYCO because the p-value for the variable was greater than 0.05.

Elevation had negative relationships with CH and NDVI for the models on the NVM, WEYCO, and GPNF management areas. The influence of elevation on CH and NDVI was significant in some cases having a coefficient of -0.56 (GPNF CH model). Elevation did however have differing effects on the WDNR management area growth. For the WDNR CH model, elevation was not significant enough to be included in the model with a p-value

>0.05. For the WDNR NDVI model, elevation had a positive relationship with NDVI values. This relationship on WDNR is inconsistent with *hypothesis 4* which stated that elevation would negatively affect growth. However, *hypothesis 4* applies to the growth present on NVM, WEYCO, and WDNR management areas.

The distance from crater variable had positive relationships with NDVI and CHM values in models where the relationship was reliable, but the variable had to be excluded from the GPNF CH and WEYCO NDVI models due to p-values greater than 0.05. Distance from crater was most significant in the NVM NDVI model with a coefficient of 0.45, but the variable had a coefficient of less than 0.15 in the remaining models. The results mirror *hypothesis 5* which states that growth would be greater further away from the crater, but this hypothesis does not apply to the GPNF CH and WEYCO NDVI models.

The NDVI and CH regression models mostly had similar relationships with the independent variables, but there were some exceptions. The independent variables were able to explain much more of the variation in CH on WEYCO (adjusted $R^2 = 0.40$) than NDVI (adjusted $R^2 = 0.20$). The same effect was seen with the regression models for NVM, except the roles were reversed. The independent variables explained less of the variation in CH (adjusted $R^2 = 0.31$) than NDVI. The NVM NDVI regression model explained the most variation in NDVI and performed better than any of the other regression models with an adjusted R^2 of 0.49.

4.6 Conclusion

This study found that slope, hillshade, and volcanic ash depth have had a significant impact on growth as measured with the CHM and NDVI in all the management areas in the MSH BZ. The thickness of ash as mapped directly following the eruption has negatively

affected growth. In areas with thicker ash deposits, growth is not as advanced in terms of both height and spectral responses to NDVI. While steeper slopes may have shown to have a negative effect on vegetation establishment in other areas, in the MSH BZ, growth is more advanced on steeper slopes. Growth on steeper slopes is more advanced in terms of both NDVI and CH on every property except GPNF where CH was not significantly related to slope, but NDVI was. The relationships with both ash depth and slope were likely different for planted v.s. non-planted areas. Vegetation on steep slopes in the NVM was relieved of ash faster due to the faster weathering in these locations, so vegetation that did survive spread in these locations. Areas that had been replanted were more likely to establish a root structure as ash was more rapidly weathered and soil availability was more abundant. Hill shade, a variable commonly known to affect growth of plants and trees maintains that relationship throughout the BZ. Areas with Higher exposure to sun had both higher NDVI and CH. Therefore, we can conclude that a steeper slope with a lower historical ash depth located in a position which allows for greater sun exposure is a prime area for vegetation growth on all management areas at MSH.

The average CH on WEYCO (52.3 ft) and WDNR (42.0 ft) was greater than that of GPNF (32.6 ft) and NVM (13.0 ft), but NVM holds the greatest CH value of 287.9 ft. Additionally, 85% of the CHM that is over 200 ft lies on the NVM. This height is not uncommon in conifer stands in the Pacific Northwest. Conifer species such as Douglas Fir, Western Hemlock, and Western Red Cedar routinely grow above 200 ft (Bingham & Sawyer 1991). In some cases, Douglas Fir has been found to grow to over 320 ft, but this height is only achieved in old growth stands at least 100 years of age or older (Sillett et al., 2021). Therefore, we can conclude that the NVM has preserved the most (0.0006 km^2) of

these old growth forest stands and fulfilled its' role as a property built to preserve.

4.7 References

Ackermann, F. (1999). Airborne laser scanning—present status and future expectations. *ISPRS Journal of Photogrammetry and Remote Sensing*, *54*(2–3), 64–67. https://doi.org/10.1016/s0924-2716(99)00009-x

Agbeshie, A. A., & Abugre, S. (2021). Soil properties and tree growth performance along a slope of a reclaimed land in the rain forest agroecological zone of Ghana. *Scientific African*, *13*. https://doi.org/10.1016/j.sciaf.2021.e00951

Bazdaric, K., Sverko, D., Salaric, I., Martinovic, A., & Lucijanic, M. (2021). The ABC of linear regression analysis: What every author and editor should know. *European Science Editing*, *47*. https://doi.org/10.3897/ese.2021.e63780

Bingham, B. B., & Sawyer J.O. (1991). Canopy Structure and tree condition of young, mature, and old-growth Douglas-Fir/Hardwood Forests. Proceedings of the Symposium on Biodiversity of Northwestern California, October 28-30, Santa Rosa, California https://www.fs.usda.gov/psw/publications/rsl/bingham3.pdf

Camarretta, N., Harrison, P. A., Bailey, T., Potts, B., Lucieer, A., Davidson, N., & Hunt, M. (2019). Monitoring Forest structure to guide adaptive management of Forest Restoration: A review of Remote Sensing approaches. *New Forests*, *51*(4), 573–596. https://doi.org/10.1007/s11056-019-09754-5

FAO. (2025). *Terms and Definitions*. Global Forest Resources Assessments | Food and Agriculture Organization of the United Nations. https://www.fao.org/forest-resources-assessment/en/

Fassnacht, F. E., White, J. C., Wulder, M. A., & Næsset, E. (2023). Remote Sensing in forestry: Current challenges, considerations and directions. *Forestry: An International Journal of Forest Research*, *97*(1), 11–37. https://doi.org/10.1093/forestry/cpad024

Fassnacht, F. E., White, J. C., Wulder, M. A., & Næsset, E. (2023a). Remote Sensing in forestry: Current challenges, considerations and directions. *Forestry: An International Journal of Forest Research*, *97*(1), 11–37. https://doi.org/10.1093/forestry/cpad024

Frenzen, P.M., 1992. Mount St. Helens– a laboratory for research and education. Journal of Forestry, 90, 14–18.

Gadow, K. v., Zhang, C. Y., Wehenkel, C., Pommerening, A., Corral-Rivas, J., Korol, M., Myklush, S., Hui, G. Y., Kiviste, A., & Zhao, X. H. (2011). Forest structure and Diversity. *Managing Forest Ecosystems*, 29–83. https://doi.org/10.1007/978-94-007-2202-6_

Hagolle, O., Colin, J., Coustance, S., Kettig, P., D'Angelo, P., Auer, S., Doxani, G., & Desjardins, C. (2021). Sentinel-2 surface reflectance products generated by CNES and DLR: Methods, validation and applications. *ISPRS Annals of the Photogrammetry, Remote Sensing and Spatial Information Sciences*, *V-1–2021*, 9–15. https://doi.org/10.5194/isprs-annals-v-1-2021-9-2021

Holland, P. G., & Steyn, D. G. (1975). Vegetational responses to latitudinal variations in slope angle and Aspect. *Journal of Biogeography*, *2*(3), 179. https://doi.org/10.2307/3037989

Kelly, M., Su, Y., Di Tommaso, S., Fry, D., Collins, B., Stephens, S., & Guo, Q. (2017). Impact of error in lidar-derived canopy height and canopy base height on modeled wildfire behavior in the sierra Nevada, California, USA. *Remote Sensing*, *10*(1), 10. https://doi.org/10.3390/rs10010010

Kok, B., & van Loenen, B. (2005). How to assess the success of National Spatial Data Infrastructures? *Computers, Environment and Urban Systems*, *29*(6), 699–717. https://doi.org/10.1016/j.compenvurbsys.2004.02.001

Lawrence, Rick & Ripple, William. (2000). Fifteen Years of Revegetation of Mount St. Helens: A Landscape-Scale Analysis. Ecology. 81. 10.2307/177338.

Lipman, P. W., & Mullineaux, D. R. (1981). The 1980 eruptions of Mount St. Helens, Washington. *Professional Paper*. https://doi.org/10.3133/pp1250

Ma, T., Zhang, C., Ji, L., Zuo, Z., Beckline, M., Hu, Y., Li, X., & Xiao, X. (2024). Development of forest aboveground biomass estimation, its problems and future solutions: A Review. *Ecological Indicators*, *159*, 111653. https://doi.org/10.1016/j.ecolind.2024.111653

Najafifar, A., Hosseinzadeh, J., & Karamshahi, A. (2019). The role of Hillshade, aspect, and toposhape in the woodland dieback of arid and semi-arid ecosystems: A case study in Zagros woodlands of Ilam Province, Iran. *Journal of Landscape Ecology*, *12*(2), 79–91. https://doi.org/10.2478/jlecol-2019-0011

Nurhidayat, M. Z., Aditya, T., Zannah, A. L., & Firdausia, S. (2023). Modelling above-ground biomass estimation using combination of vegetation height and forest canopy density at secondary peat swamp forest of Kalimantan. *IOP Conference Series: Earth and Environmental Science*, *1276*(1), 012001. https://doi.org/10.1088/1755-1315/1276/1/012001

Oh, S., Jung, J., Shao, G., Shao, G., Gallion, J., & Fei, S. (2022). High-resolution canopy height model generation and validation using USGS 3DEP Lidar Data in Indiana, USA. *Remote Sensing*, *14*(4), 935. https://doi.org/10.3390/rs14040935

Ozili, P. K. (2022). The acceptable R-square in Empirical Modelling for Social Science Research. *SSRN Electronic Journal*. https://doi.org/10.2139/ssrn.4128165

Primicia, I., Camarero, J. J., Janda, P., Čada, V., Morrissey, R. C., Trotsiuk, V., Bače, R., Teodosiu, M., & Svoboda, M. (2015). Age, competition, disturbance and elevation effects on tree and stand growth response of primary picea abies forest to climate. *Forest Ecology and Management*, *354*, 77–86. https://doi.org/10.1016/j.foreco.2015.06.034

Programme of The European Union. *Sentinel 2 Level 2A*, (2017). Available via: https://dataspace.copernicus.eu/terms-and-conditions

Rahman, A. ur, Khan, S. M., Ahmad, Z., Alamri, S., Hashem, M., Ilyas, M., Aksoy, A., Dülgeroğlu, C., & Shahab Ali, G. K. (2021). -impact of multiple environmental factors on species abundance in various forest layers using an integrative modeling approach. *Global Ecology and Conservation*, *29*. https://doi.org/10.1016/j.gecco.2021.e01712

Radwan, M. A., & Campbell, D. L. (1981). Mount St. Helens Ash and mud: Chemical properties and effects on germination and establishment of trees and browse plants. *Pacific Northwest Forest and Range Experiment Station U.S.D.A.* https://doi.org/10.2737/pnw-rp-294

Senaviratna, N. A., & A. Cooray, T. M. (2019). Diagnosing multicollinearity of logistic regression model. *Asian Journal of Probability and Statistics*, 1–9. https://doi.org/10.9734/ajpas/2019/v5i230132

Sibona, E., Vitali, A., Meloni, F., Caffo, L., Dotta, A., Lingua, E., Motta, R., & Garbarino, M. (2016). Direct measurement of tree height provides different results on the assessment of Lidar Accuracy. *Forests*, *8*(1), 7. https://doi.org/10.3390/f8010007

Sillett, S. C., Kramer, R. D., Van Pelt, R., Carroll, A. L., Campbell-Spickler, J., & Antoine, M. E. (2021). Comparative development of the four tallest conifer species. *Forest Ecology and Management*, *480*, 118688. https://doi.org/10.1016/j.foreco.2020.118688

Sibona, E., Vitali, A., Meloni, F., Caffo, L., Dotta, A., Lingua, E., Motta, R., & Garbarino, M. (2016). Direct measurement of tree height provides different results on the assessment of Lidar Accuracy. *Forests*, *8*(1), 7. https://doi.org/10.3390/f8010007

U.S. Geological Survey. *Cascades South 3dep 2019,* (2019). Available via WDNR LiDAR Portal: https://lidarportal.dnr.wa.gov/

U.S. Geological Survey. *Southwest Washington Foothills,* (2017). Available via WDNR LiDAR Portal: https://lidarportal.dnr.wa.gov/

Waitt R., Hansen V., Sarna-Wojcicki A., Wood S. (1981) Proximal airfall deposits of eruptions between May 24 and August 7,1980 — stratigraphy and field sedimentology. *U.S. Geological Survey Professional Paper 1250:*617–630

Wang, S., Zhao, M., Meng, X., Chen, G., Zeng, R., Yang, Q., Liu, Y., & Wang, B. (2020). Evaluation of the effects of forest on slope stability and its implications for forest management: A case study of bailong river basin, China. *Sustainability*, *12*(16), 6655. https://doi.org/10.3390/su12166655

Wang, L., Li, Z., Gao, C., Li, J., & Cui, K. (2025). The altitude shapes the heterogeneity of tree growth by modulating the soil characteristics and microorganisms in the Calocedrus Macrolepis Plantation. *Forest Ecology and Management*, *578*, 122459. https://doi.org/10.1016/j.foreco.2024.122459

Wang, Y., Lehtomäki, M., Liang, X., Pyörälä, J., Kukko, A., Jaakkola, A., Liu, J., Feng, Z., Chen, R., & Hyyppä, J. (2019). Is field-measured tree height as reliable as believed – a comparison study of tree height estimates from field measurement, airborne laser scanning and terrestrial laser scanning in a boreal forest. *ISPRS Journal of Photogrammetry and Remote Sensing*, *147*, 132–145. https://doi.org/10.1016/j.isprsjprs.2018.11.008

Washington Department of Natural Resources. *Southwest State Lands,* (2017). Available via WDNR LiDAR Portal: https://lidarportal.dnr.wa.gov/

Xian, Y., Wang, T., Yu, P., & Du, Y. (2024). To ignore or not: Understanding the influence of hillshade. *IEEE Journal of Selected Topics in Applied Earth Observations and Remote Sensing*, *17*, 9009–9017. https://doi.org/10.1109/jstars.2024.3389829

Chapter 5: Summary and Future Work

Summary

This thesis has two chapters that are based on separate research questions. First, in chapter 3, this study utilized Emerging Hot Spot Analysis (EHSA) of time series Normalized Difference Vegetation Index (NDVI) images to make conclusions on vegetation growth at Mount St. Helens (MSH). The purpose of the EHSA was to identify specific patterns of growth which were determined using the 40-year time series collection of satellite imagery. EHSA determined patterns based off values of each pixel in the time series of images based on the temporal trend and spatial clustering of NDVI values. The Landsat Level 2 Collection 2 Surface Reflectance products used for the analysis are superior to prior Landsat Collections used at the Blast Zone (BZ). The images have a finer spatial resolution of 30 meters. The processing completed by the Landsat Ecosystem Disturbance Adaptive Processing System (LEDAPS) and Surface Reflectance Code (LASRC) processing algorithms introduce improved geolocation accuracy, radiometric correction, and atmospheric correction to ensure accuracy and consistency for analysis.

The Weyerhaeuser Timber Company (WEYCO) and Washington Department of Natural Resources (WDNR) management areas are experiencing a more inconsistent rate of growth. The Gifford Pinchot National Forest (GPNF) and particularly the National Volcanic Monument (NVM) management areas seem to be maintaining a consistent trend of growth over the 40 years. These properties hold the overwhelming majority of diminishing cold spots and new hot spots. However, the properties that have been more consistently managed (WEYCO and WDNR), including processes such as replanting conifer species, have a greater extent of initial and subsequent growth as determined by

the NDVI values. Therefore, WEYCO and WDNR management areas have the greatest extent of growth, but external disturbances have interfered with the consistency of this growth. GPNF and NVM management areas may have had the least extent of growth, but the EHSA patterns on these properties suggest these properties are growing consistently and may continue to do so without any interference.

The fourth chapter of this study aimed to explore potential drivers of revegetation at MSH. This chapter utilizes Multiple Linear Regression (MLR) to compare relationships between the dependent variables of the study area Canopy Height (CH) and NDVI to the independent variables slope, ash depth, elevation, distance from crater, and hill shade. The study found that slope, hillshade, and volcanic ash depth have had a significant impact on growth of both CH and NDVI. In areas with thicker ash deposits, growth is not as advanced in terms of both height and spectral responses to NDVI. Growth on steeper slopes is more advanced in terms of both the NDVI and CH on nearly every property. Areas with higher exposure to sun, as indicated with the hillshade variable, had greater values of NDVI and the CH. Therefore, this study can conclude that a steeper slope with a lower historical ash depth located in a position which allows for greater sun exposure is a prime area for growth at MSH.

The results from chapters 3 and 4 are key findings introducing new knowledge on the progress and characteristics of reforestation in the MSH BZ. The extensive time series of images paired with EHSA has allowed for the identification of patterns of growth that have occurred since 1984. This 40-year collection allows for a better understanding of the growth that has occurred since the eruption identifying areas of new hotspots of growth and areas where outside interference such as timber harvesting has interrupted growth.

Previous studies have had both a more coarse temporal and spatial resolution which limits the extent of possible observations that can be made with a greater time series of images and finer spatial and temporal resolution. Environmental variables identified by earlier studies at MSH were found to still influence growth even in the year 2017. Previous studies, limited to vegetation indices, were able to identify these relationships, but this study further expands on that knowledge by introducing the effect that such variables have on CH. Results were similar between both spectral responses and height responses to slope, ash depth, hillshade, elevation, and distance from crater.

Future Work

Potential future research in the area consists of exploring additional variables that may influence growth. Such variables may not have a linear relationship with growth or be continuous type data. Therefore, methods such as regression tree analysis could be introduced to explore these relationships. Additionally, utilizing the time series of NDVI images, there are climatic factors that could have introduced growth, especially in earlier years. Identifying periods of drought or especially brutal winters may help better understand what effected initial growth.

Appendix A: Data Access

Use	Data Type	Location
BZ Boundary	Polygon	https://doi.org/10.1080/10106049.2011.584977
Management Area Boundaries	Polygon	https://doi.org/10.1080/10106049.2011.584977 https://geo.wa.gov/
Landsat Level 2 collection 2 NDVI	Raster	https://earthexplorer.usgs.gov/
Sentinel Level 2 Collection 2 NDVI	Raster	https://dataspace.copernicus.eu/explore-data/data-collections/sentinel-data/sentinel-2
ALS Derived DTM	Raster	https://lidarportal.dnr.wa.gov/#46.40504:-122.16888:9
ALS Derived DSM	Raster	https://lidarportal.dnr.wa.gov/#46.40504:-122.16888:9
ALS Derived Hillshade	Raster	https://lidarportal.dnr.wa.gov/#46.40504:-122.16888:9
Crater Location	Point	https://doi.org/10.3133/pp1250
Ash Depth	Raster	https://scholarworks.boisestate.edu/geo_facpubs/160/